Sorrento SAPEM'23 常熟

7th Symposium on the Acoustics of Poro-Elastic Materials

第七届多孔弹性材料声学技术大会

Preparation, Acoustic Absorption and Application Prospect of Aerogels

气凝胶材料的研制、吸声性能与应用前景

Dr. Ju-Qi Ruan （阮居祺 博士 / 硕导）

School of Physics Science and Technology

Kunming University, Yun Nan, China

Nov. 7, 2023

Outline

1. Research Background

2. Acoustic Absorption Characteristics of Inorganic Aerogels —— SiO_2 Aerogel

3. Acoustic Absorption Characteristics of Organic Aerogels —— Bio-based Aerogel (cellulose)

4. Summary and Outlook

1. Research Background

► Noise problem !

High-end equipment manufacturing

Constructions

Daily life

▶ How to eliminate noise ?

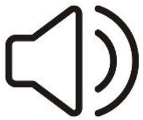

1. Sound source

2. Propagation path

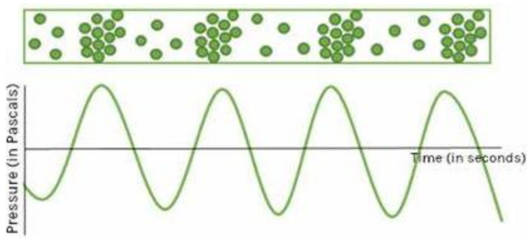

Sound-absorbing materials

3. Human ears

▶ Sound-absorbing materials

Porous material [1]

Nat. Commun. (2014)

(Micro-) perforated plate

Metamaterial [2]

Nat. Mater. (2014)

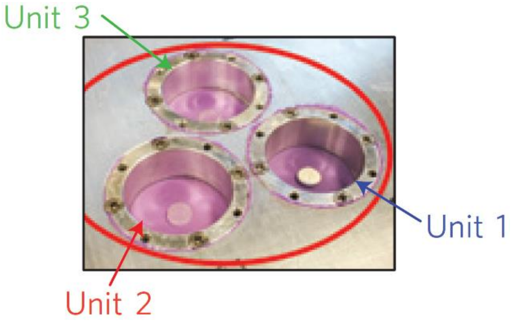

Hybrid type [3]

Mater. Horiz. (2017)

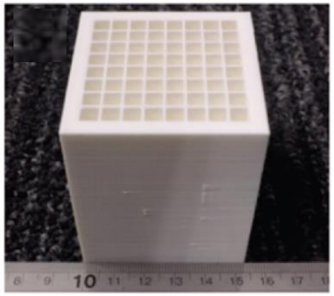

Comparison of each type of sound-absorbing material

	Bandwidth (for absorption)	Designability (to frequency)	Cost	Sustainability	Space saving
Porous material	★★★	★	★★★★	★★★★	★★★★
(Micro-) perforated plate	★	★★★	★★★	★★★	★
Metamaterial	★★	★★★★	★★	★★	★★
Hybrid type	★★★★	★★	★	★★	★★

▶ Porous sound-absorbing materials

Aerogels

1. **Metal-based** (Metal foams [4], etc.)
2. **Inorganic species** (Ceramic foams [5], Rock wool, etc.)
3. **Organic species** (Polymer foams [6], etc.)
4. **Composites** (MOFs, etc.)

[4] J. A. Liu, et al., *J. Mater. Res. Technol.*, **25:** 1263-1272 (2023)

[5] J. Y. Lou, et al., *Ceram. Int.*, **49:** 38103-38114 (2023)

[6] R. Y. Cai, et al., *ACS Appl. Polym. Mater.*, **5:** 7795-7804 (2023)

Aerogels

Broke 15 Guinness World Records:

1. **Lowest density** (solid, < 1.5 mg/cm^3)
2. **Lowest sound speed**
3. **Highest porosity** (up to 99.9%)
4. Minimum aperture
5. Widest range of density
6. Highest acoustic impedance
7. Lowest refractive index (to light, < 1.0003)
8. Widest range of refractive index (to light)
9. Lowest Young's modulus
10. Lowest loss angle tangent (< 10^{-4})
11. Lowest dielectric constant (< 1.003)
12. Widest range of compression modulus
13. Lowest thermal conductivity (< 0.013 W/(mK))
14. Most loose structural material for 3D printing
15. 1st implementation of sampling from the comet

1st generation — Inorganic aerogel
(Typical: **SiO_2 aerogel**)

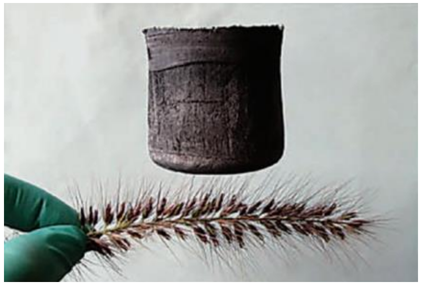

Adv. Mater. (2013)

2nd generation — Organic polymer aerogel
(Typical: Carbon-based aerogel [7])

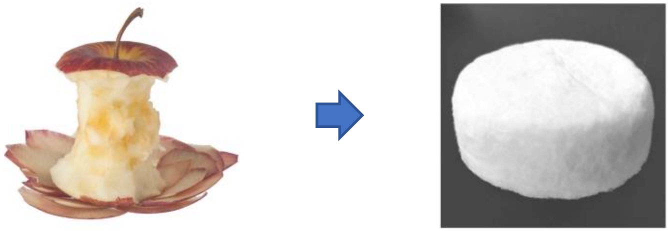

3th generation — Bio-based aerogel
(Typical: **Cellulose aerogel**)

2. Acoustic Absorption Characteristics of Inorganic Aerogels

(SiO_2 Aerogel)

Combining advantages

"Lightweight and high-strength" & "High-efficiency acoustic absorption"

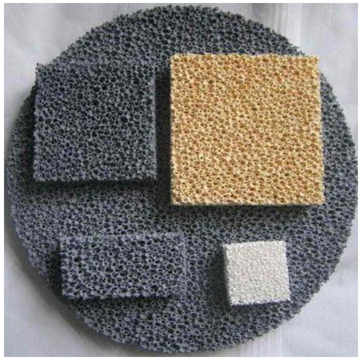

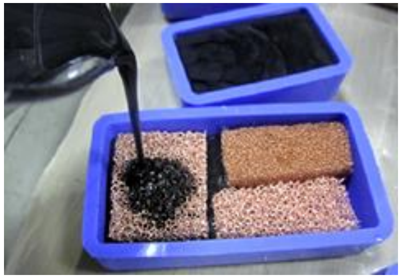

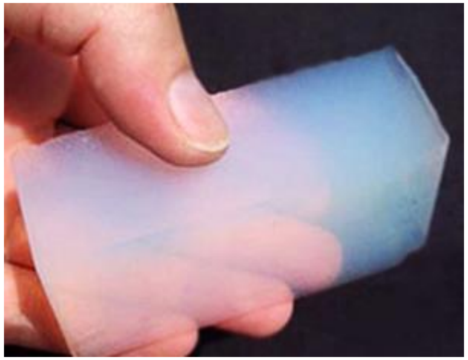

Metal foam
(primary structure)

Bimodal structure

Aerogel
(secondary structure)

High specific stiffness

Metal foam/Aerogel Composites

High acoustic damping

Work 1: Acoustic absorption performance of Copper Foam/SiO_2 Aerogels (CFSAs) and Iron Foam/SiO_2 Aerogel (IFSA) composites

Ju-Qi Ruan, et al., *AIP Adv.*, 9: 015209 (2019)

Ju-Qi Ruan, et al., *Appl. Phys. Express*, 12: 035002 (2019) **（编辑荐读精选文章）**

发明专利：卢明辉、阮居祺、李政、张善涛、陈延峰，ZL 2015 1 0810252. 5

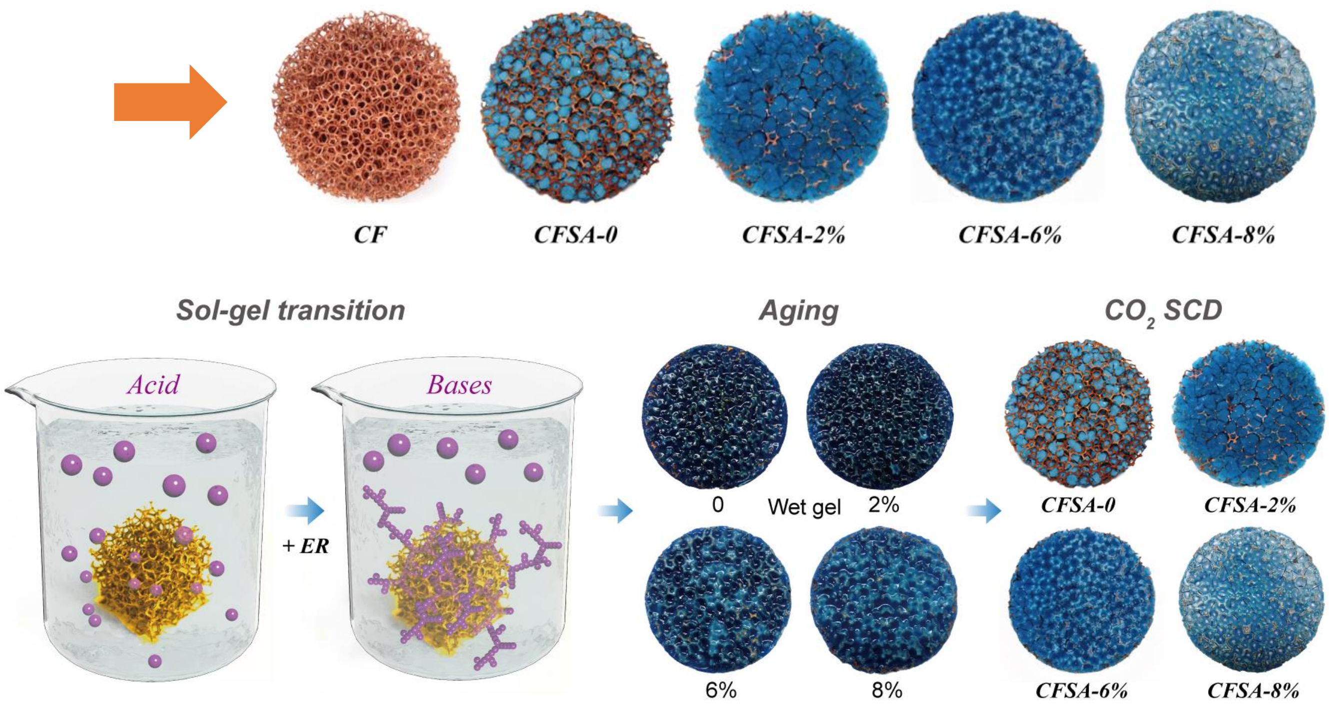

CFSAs

Fig. 1. Fabrication of bimodal CFSAs through a two-step, acid-base catalyzed sol-gel transition followed by *CO_2 supercritical drying* process.

- **High cost** (e.g., copper foam、CO_2 SCD)
- **Complicated procedures** (e.g., + epoxy resin)
- **Low mechanical strength**

IFSA

wt.%$_{(SA)}$ = 32.69%

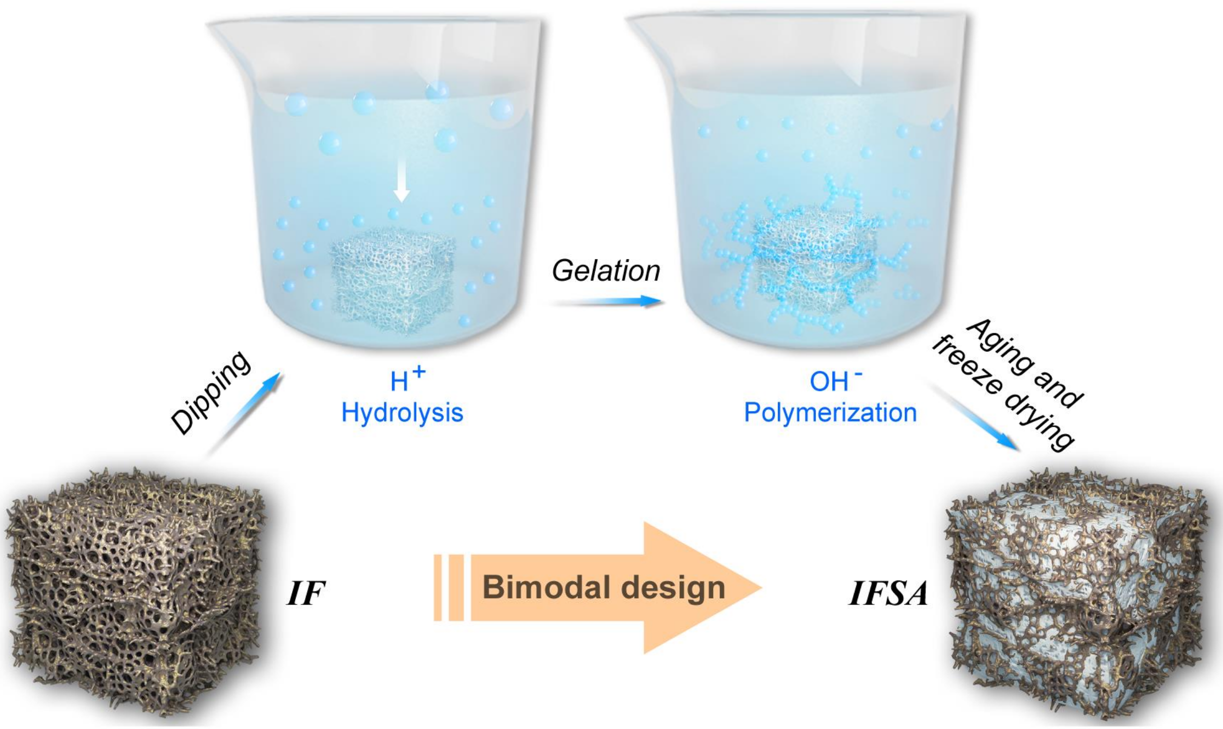

Fig. 2. Preparation of bimodal IFSA through a two-step, acid-base catalyzed sol-gel transition, afterwards dried by *freeze drying*.

Iron foam

(Porosity: 98±1%; 250 ppi)

IFSA

(High morphology integrity)

Johnson–Champoux–Allard (JCA) Combined with Bimodal Model

JCA Model [8] J. Acoust. Soc. Am. (2017)

$$\rho_e(\omega)=\frac{\alpha_\infty\rho_0}{\phi}\left(1+\frac{r_s\phi}{i\omega\rho_0\alpha_\infty}\sqrt{1+\frac{4i\alpha_\infty^2\eta\rho_0\omega}{r_s^2\Lambda^2\phi^2}}\right)$$

$$K_e(\omega)=\frac{\gamma p_0}{\phi}\left[\gamma-(\gamma-1)\left(1+\frac{8\eta}{i\Lambda'^2N_{pr}\omega\rho_0}\sqrt{1+\frac{i\rho_0\omega N_{pr}\Lambda'^2}{16\eta}}\right)^{-1}\right]^{-1}$$

$$\Lambda=\frac{1}{c}\sqrt{\frac{8\alpha_\infty\eta}{\phi r_s}} \qquad \Lambda'=\frac{1}{c'}\sqrt{\frac{8\alpha_\infty\eta}{\phi r_s}}$$

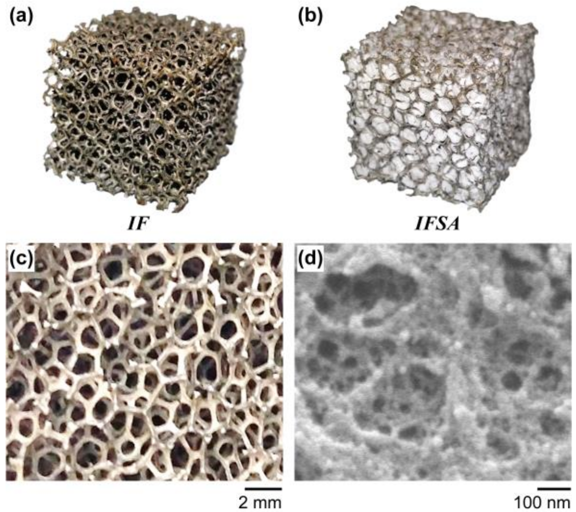

(**Bimodal structure** of IFSA)

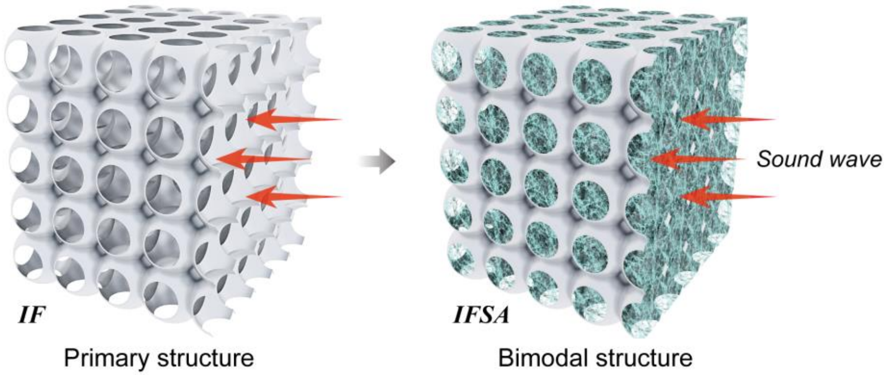

Designed Bimodal Model (3D)

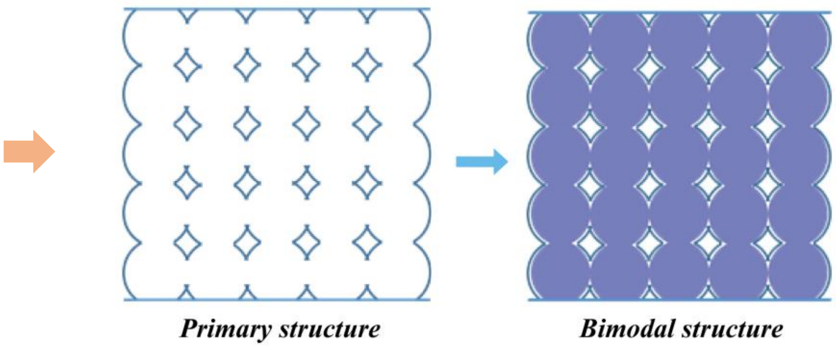

Designed Bimodal Model (2D)

Acoustic absorption performance of CFSAs

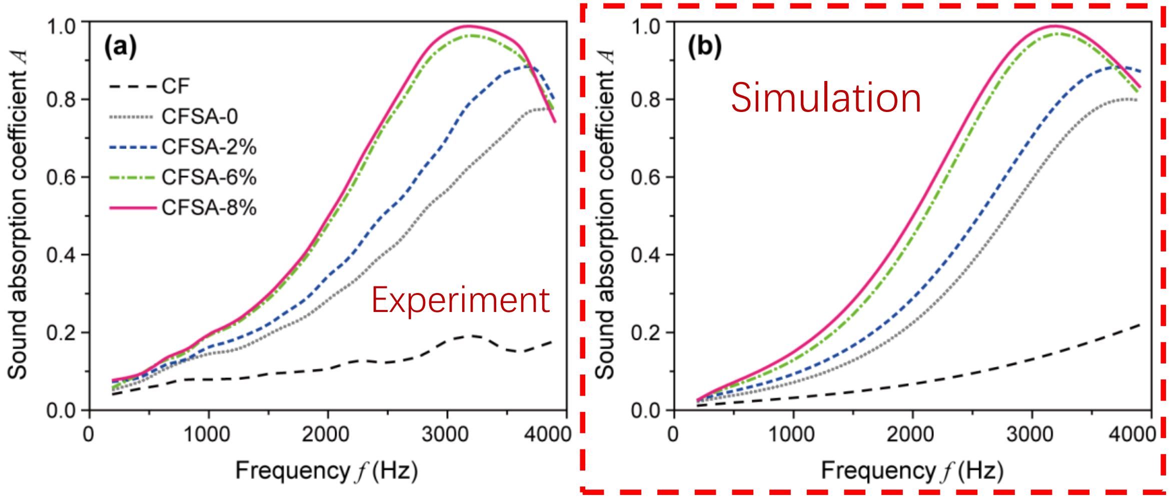

Fig. 3. Normal incident sound absorption coefficient of CF and CFSAs: (a) Experimental measurements. (b) Simulation results from the designed bimodal model.

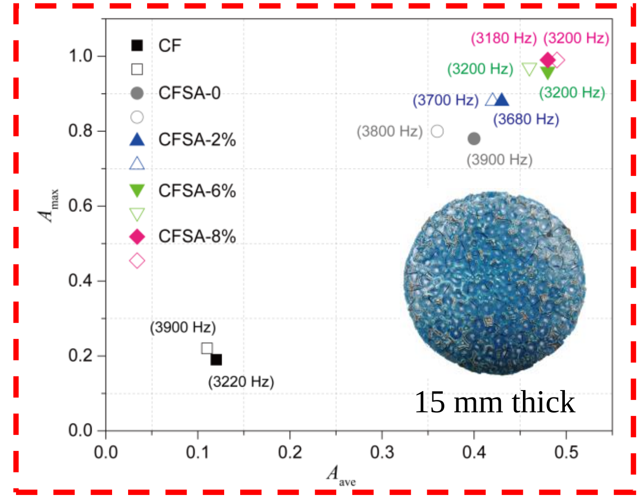

Fig. 4. Maximum and average sound absorption coefficient of CF and CFSAs.

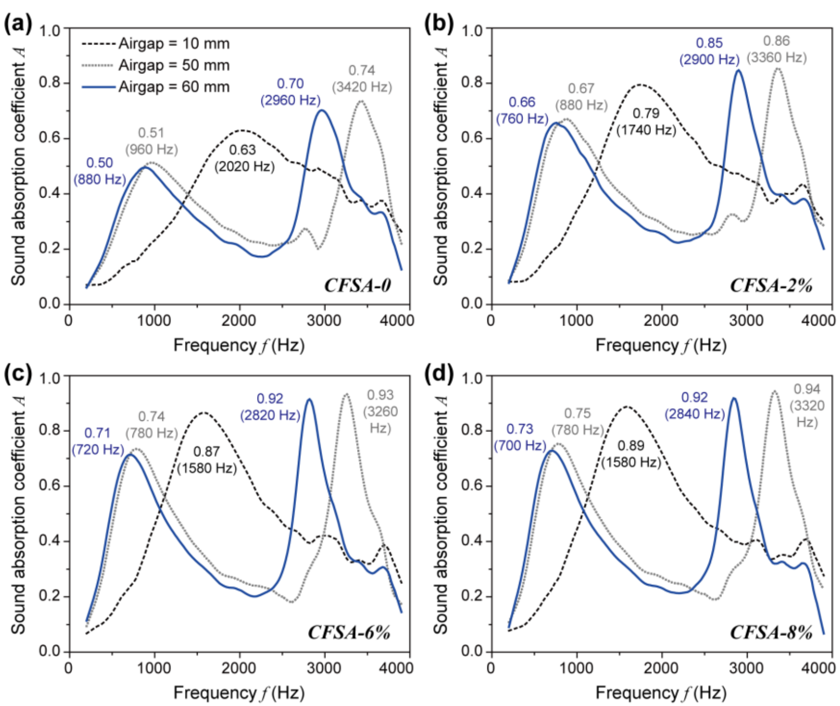

Table. 1. Porosity and static airflow resistivity of CF and CFSAs

Sample	CF	CF-0	CFSA-2%	CFSA-6%	CFSA-8%
Porosity (%)	97.03	94.10	92.64	91.50	90.50
Airflow resistivity (N·s/m^4)	210	1100	1800	2600	6200

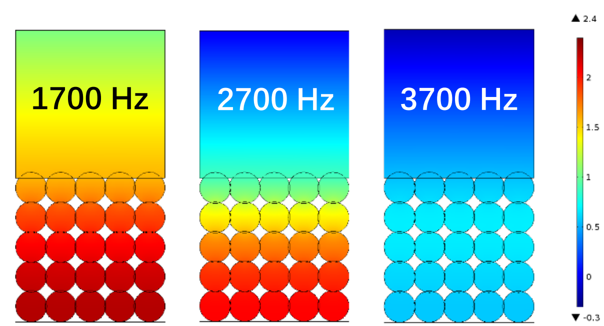

Total Acoustic Pressure Field of CFSA-8%

Acoustic absorption performance of IFSA

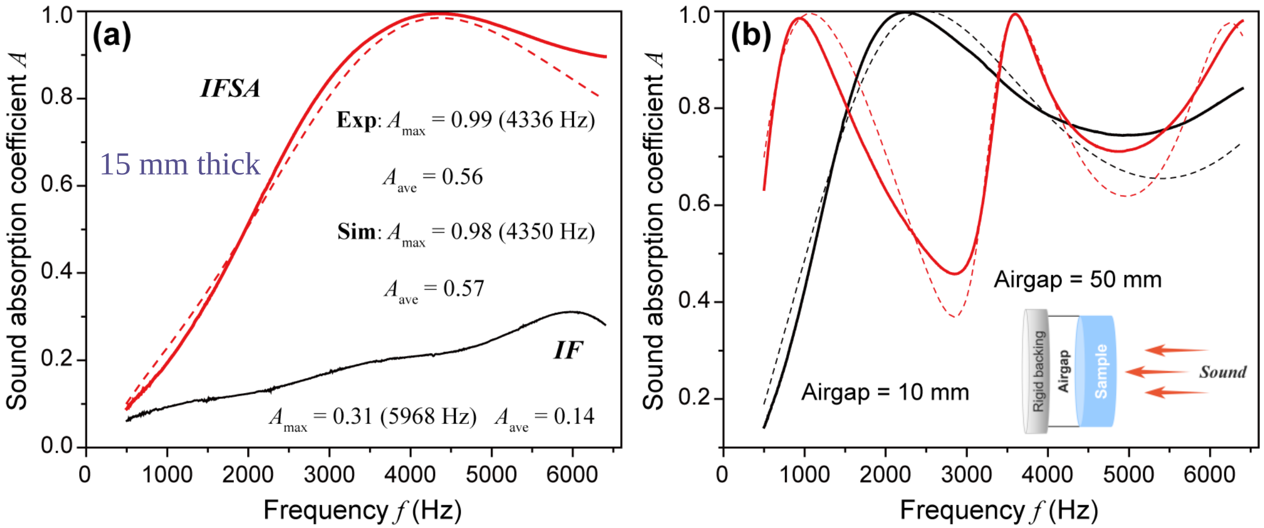

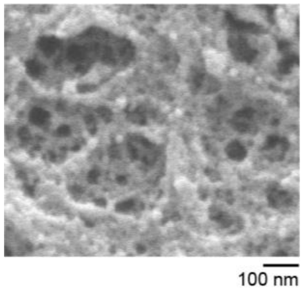

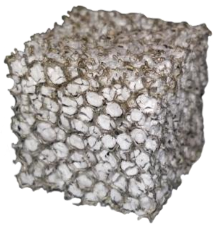

IFSA

Fig. 5. (a) Normal incident sound absorption coefficient of IF and IFSA. (b) Effect of the airgap thickness on low-frequency sound absorption properties of IFSA.

Porosity (%): **95.31** (±1)

Airflow resistivity (N·s/m^4) **20262.27** (±1329.26)

Tortuosity: 1.5 (±0.05)

Viscous length (μm) **93.26** (±2)

Thermal length (μm) **186.52** (±2)

Table. 2. Maximum sound absorption coefficient and its corresponding frequency of IFSA with different airgap thickness

Airgap thick	First		First (Hz)		Second		Second (Hz)	
	Exp	**Sim**	Exp	**Sim**	Exp	**Sim**	Exp	**Sim**
10 mm	0.99	0.99	2240	2500	—	—	—	—
50 mm	0.99	0.99	956	1050	0.99	0.99	3596	3600

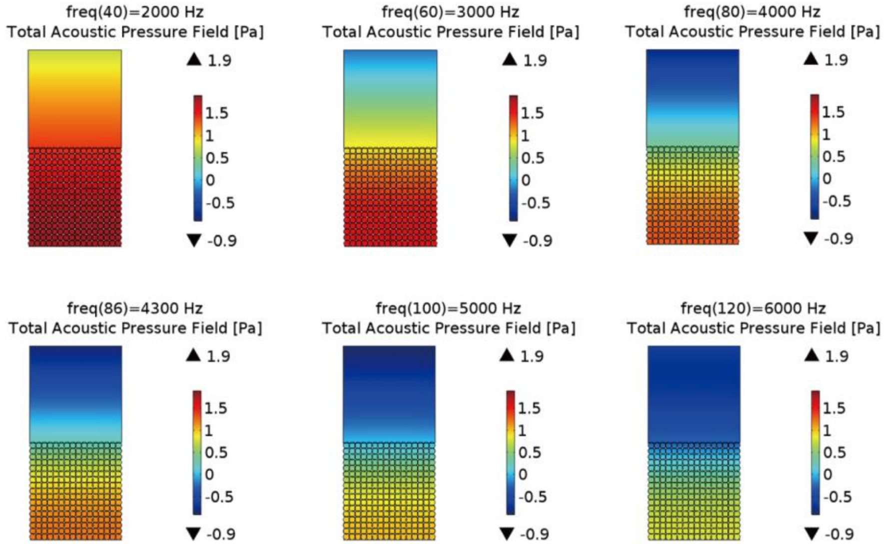

Total Acoustic Pressure Field

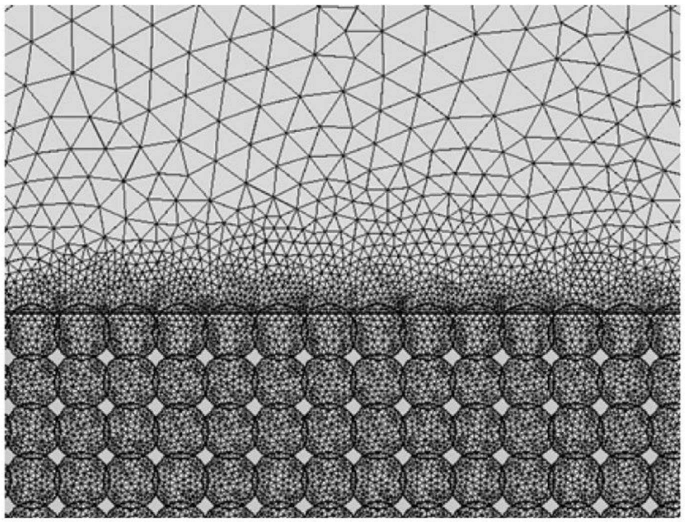

Free triangular mesh

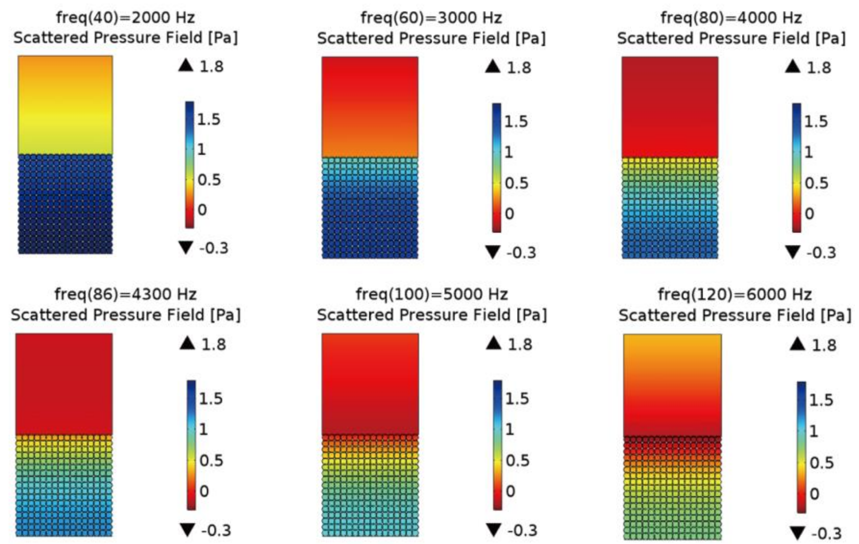

Scattered Pressure Field

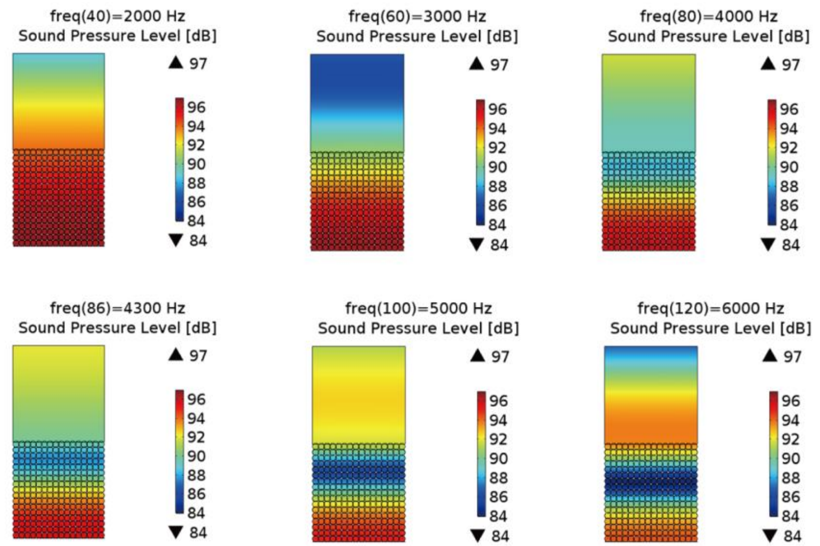

Sound Pressure Level

Mechanical properties of CFSAs & IFSA

Compression behavior of CFSAs

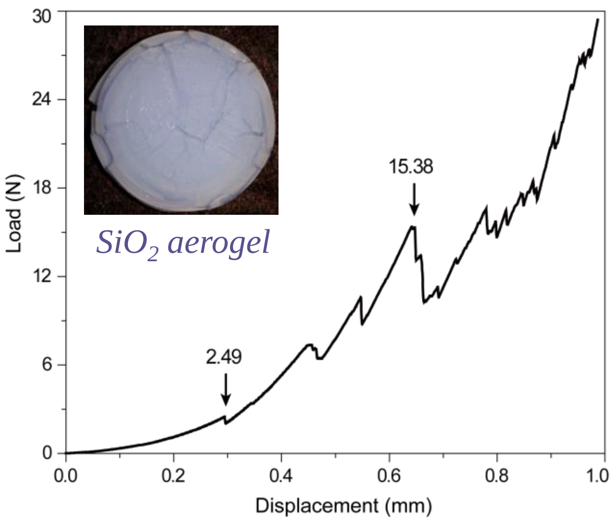

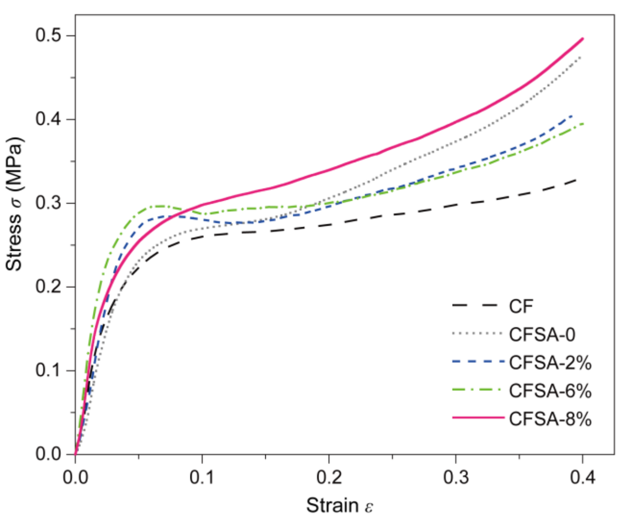

Compression behavior of IFSA

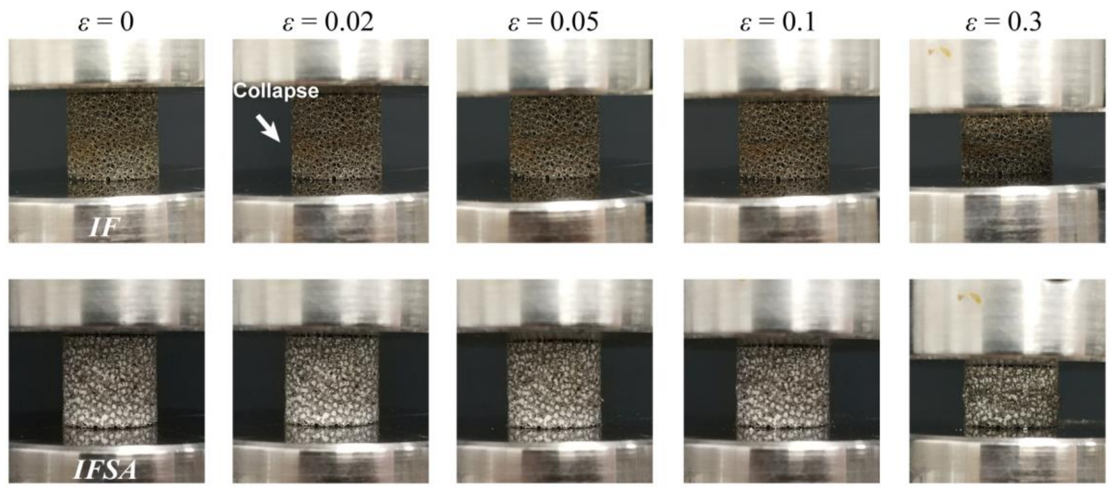

' Axial quasi-static compression '

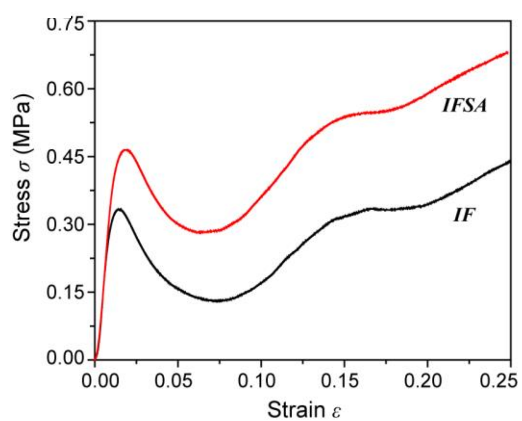

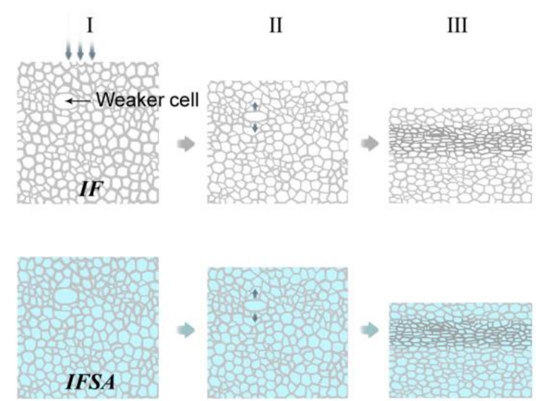

(Deformation mechanism)

Density and parameters of compression properties of CF, IF, CFSAs and IFSA

Sample	CF	CFSA-0	CFSA-2%	CFSA-6%	CFSA-8%	IF	IFSA
Young's modulus (MPa)	7.89	7.12	8.12	11.01	9.99	46.49 (±4.38)	46.6 (±3.94)
Compression strength (MPa)	0.25	0.26	0.28	0.30	0.26	0.33 (±0.01)	0.46 (±0.04)
Density (g/cm^3)	0.20	0.26	0.26	0.28	0.28	0.19 (±0.01)	0.29 (±0.01)
Specific modulus ($10^5\ m^2/s^2$)	0.39	0.27	0.31	0.39	0.36	2.4 (±0.3)	1.6 (±0.1)

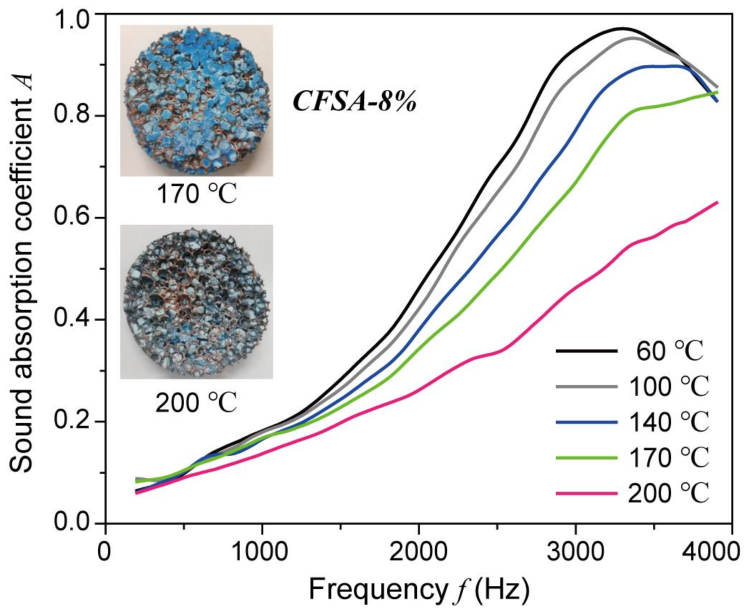

Temperature resistance

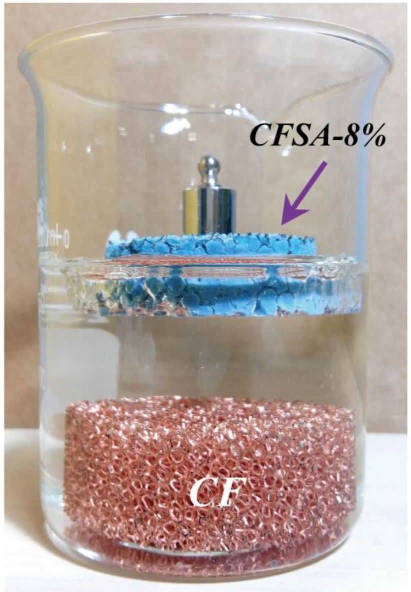

Hydrophobicity

Sample Presentation


Copper foam


Nickel foam


Iron foam


SiO_2 aerogel


RF aerogel

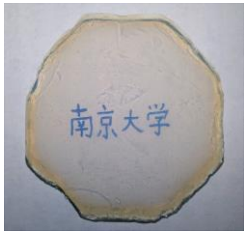

Al-Si aerogel (Transparent)

Combination

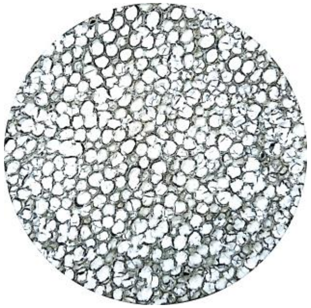
Iron foam/SiO_2 Aerogel


Copper foam/SiO_2 Aerogel


Nickel foam/SiO_2 Aerogel

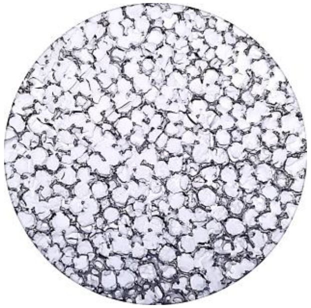
Nickel foam/(flexible) SiO_2 Aerogel


Iron foam/RF Aerogel

3. Acoustic Absorption Characteristics of Organic Aerogels

(Bio-based Aerogel (cellulose))

Work 2: Acoustic absorption performance of Natural Cellulose Nanocrystal Aerogels (CNCAs)

Ju-Qi Ruan, et al., *AIP Adv.*, 12: 055102 (2022)

Ju-Qi Ruan, et al., *J. Mater. Sci*, 58: 971-982 (2023) （编辑荐读精选文章）

Facile Low-cost Green

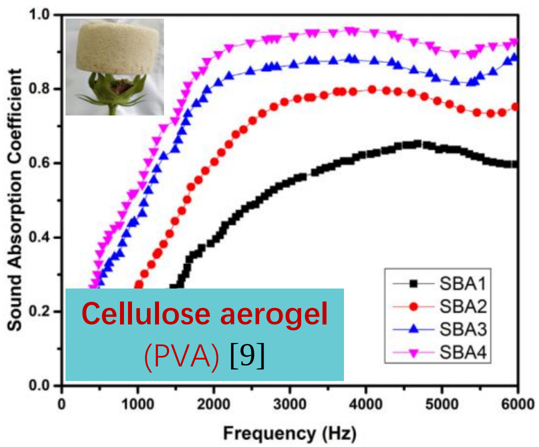

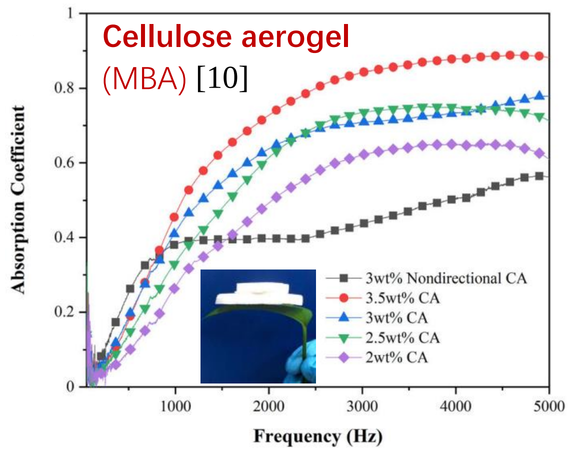

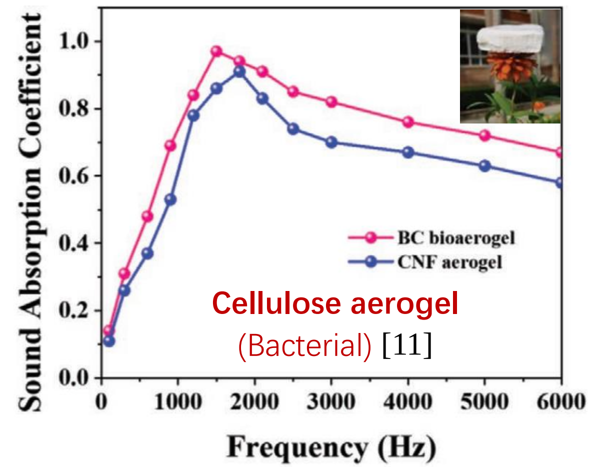

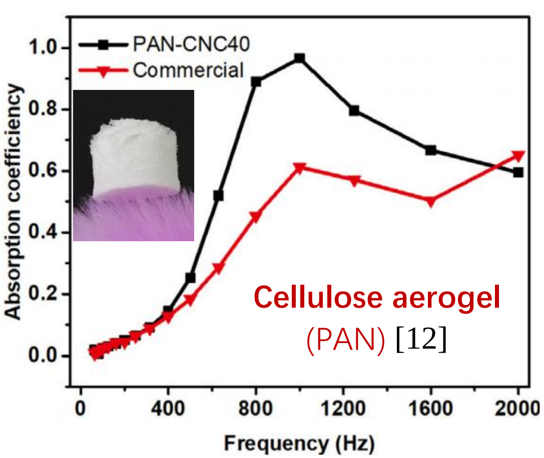

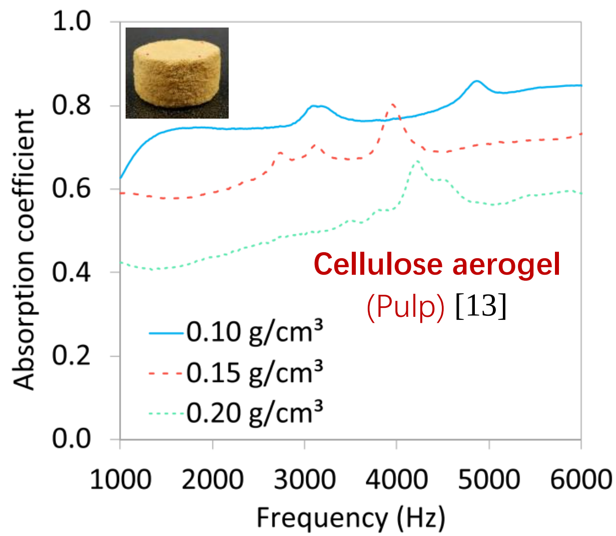

[9] G. Kumar, et al., *J. Cleaner Prod.*, **298:** 126744 (2021)

[10] C. W. Lou, et al., *J. Mater. Sci.*, **56:** 18762–18774 (2021)

[11] Z. Cheng, et al., *Adv. Mater. Interfaces*, **8:** 2002101 (2021)

[12] L. T. Cao, et al., *J. Colloid Interface Sci.*, **597:** 21-28 (2021)

[13] I. Hafes, et al., *ACS Sustainable Chem. Eng.*, **9:** 10113-10122 (2021)

Sample Preparation (CWs)

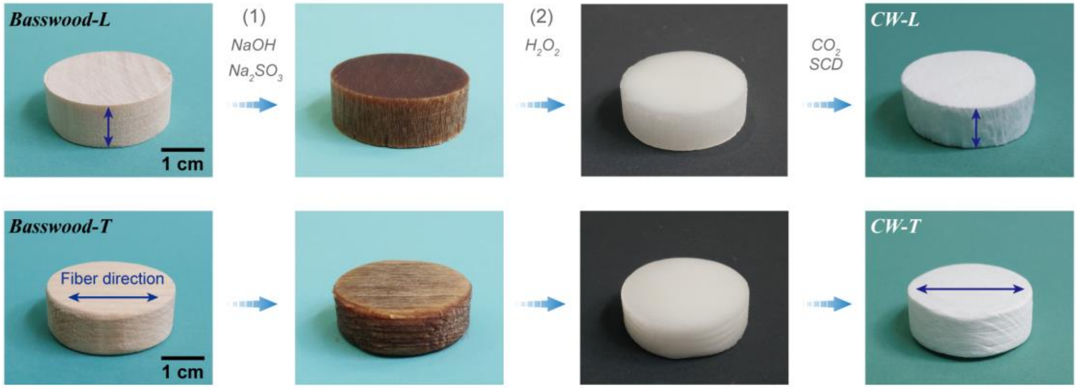

Fig. 6. Preparation of CWs along the longitudinal and tangential directions via a two-step lignin removal process followed by supercritical CO_2 drying.

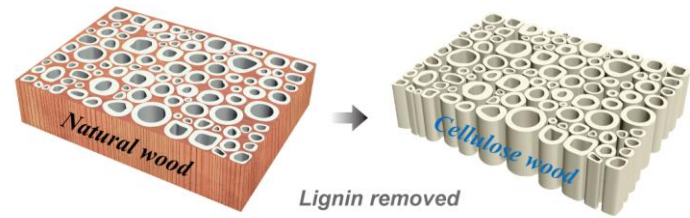

'preparation principle'

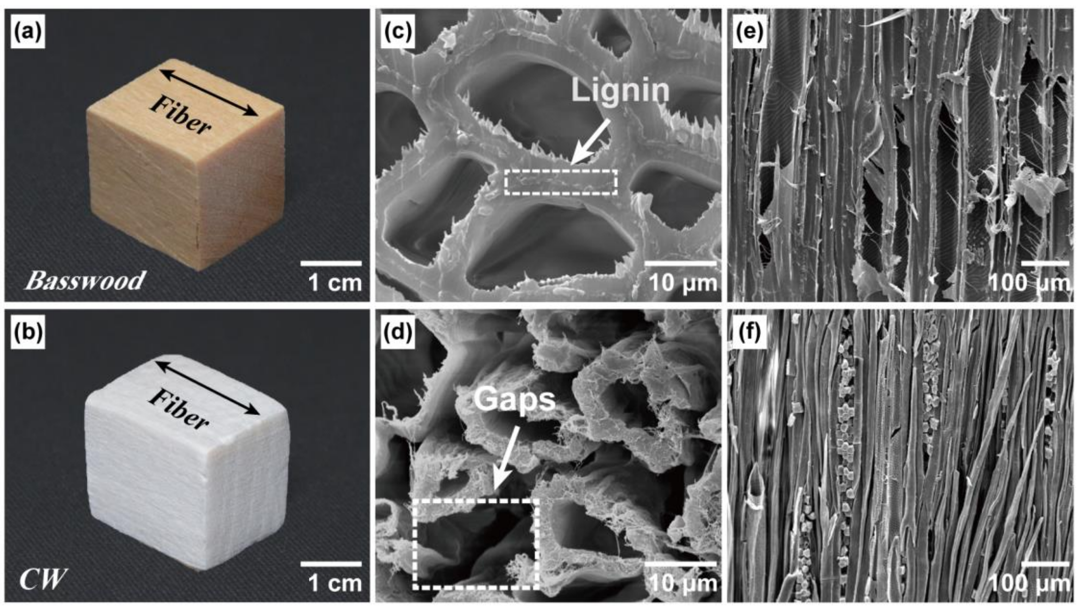

Fig. 7. Optical images of natural basswood matrix (a) and the as-prepared CW (b). SEM images of natural basswood (c, e) and CW (d, f).

Samples for acoustic absorption measurement

Basswood-T CW-T

Basswood-L CW-L

Sample Preparation (CNCAs)

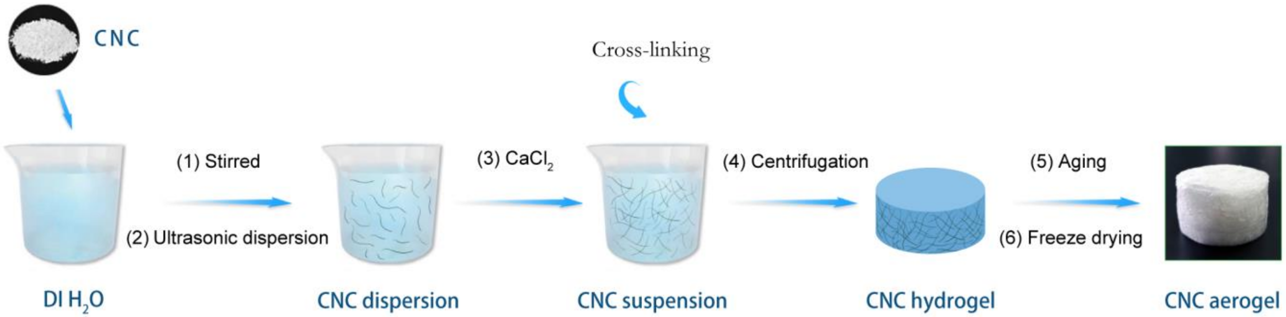

Fig. 8. Schematic illustration of the preparation process of the cellulose nanocrystal (CNC) aerogels.

Green

Sustainable

Low Cost

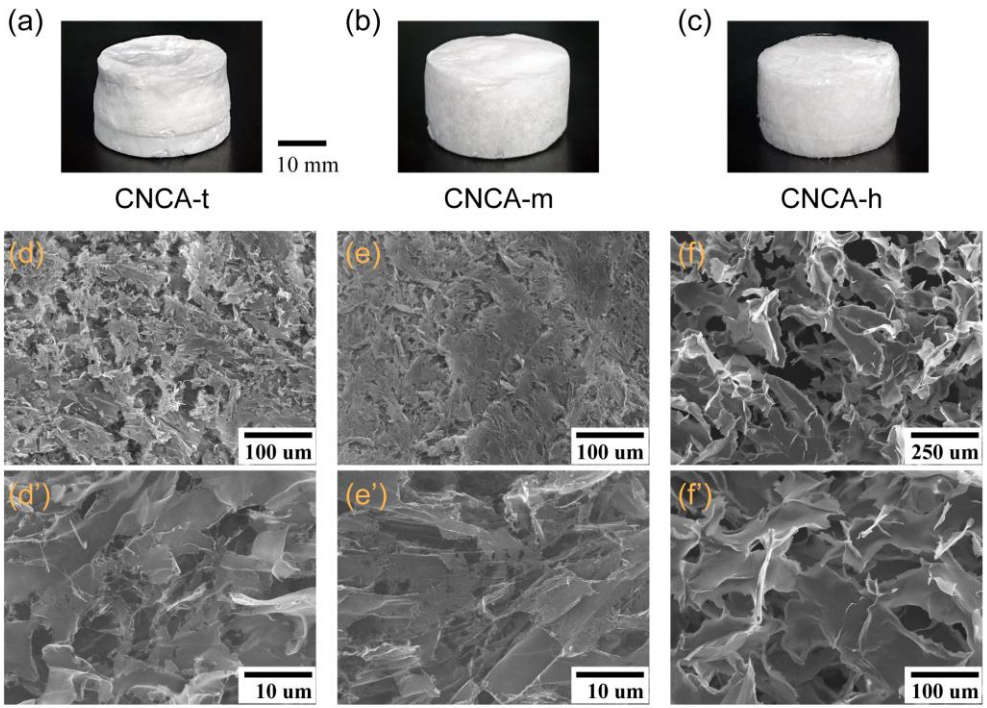

Fig. 9. Optical photographs (a-c) and SEM images of CNC aerogels. d and d', e and e', f and f' show the morphology of CNCA-t, CNCA-m, and CNCA-h at low and high magnification, respectively.

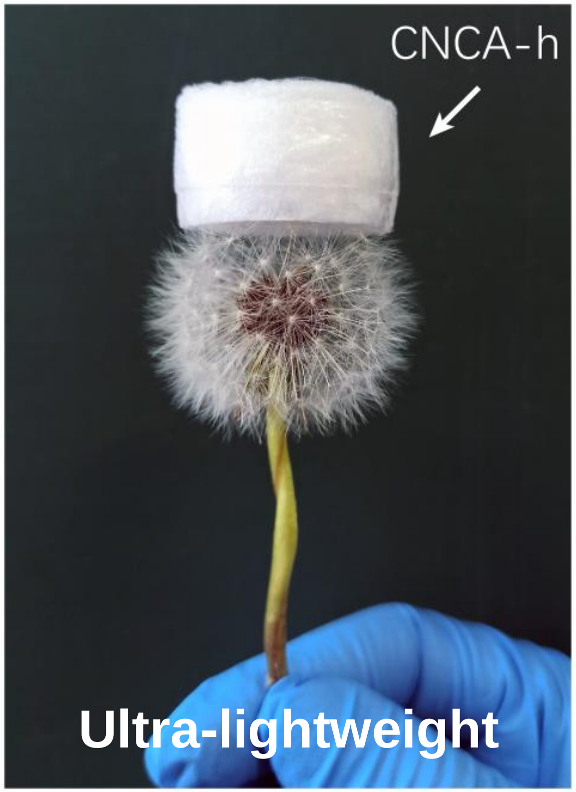

Three-parameter Approximate Johnson-Champoux-Allard-Lafarge (JCAL) Model

$\phi \quad \alpha_\infty$

$\Lambda \quad \Lambda'$

$\kappa_0 \quad \kappa_0'$

$$\kappa_0 = \frac{\bar{s}^2 \phi}{8\alpha_\infty} e^{-6(\sigma_s \log 2)^2} \qquad \kappa_0' = \frac{\bar{s}^2 \phi}{8\alpha_\infty} e^{6(\sigma_s \log 2)^2}$$

$$\Lambda = \bar{s} e^{-5/2(\sigma_s \log 2)^2} \qquad \Lambda' = \bar{s} e^{3/2(\sigma_s \log 2)^2}$$

$$\alpha_\infty = e^{4(\sigma_s \log 2)^2}$$

[14] *J. Acoust. Soc. Am.* (2019)

[15] *J. Acoust. Soc. Am.* (2016)

ϕ

$\bar{s}$

σ_s

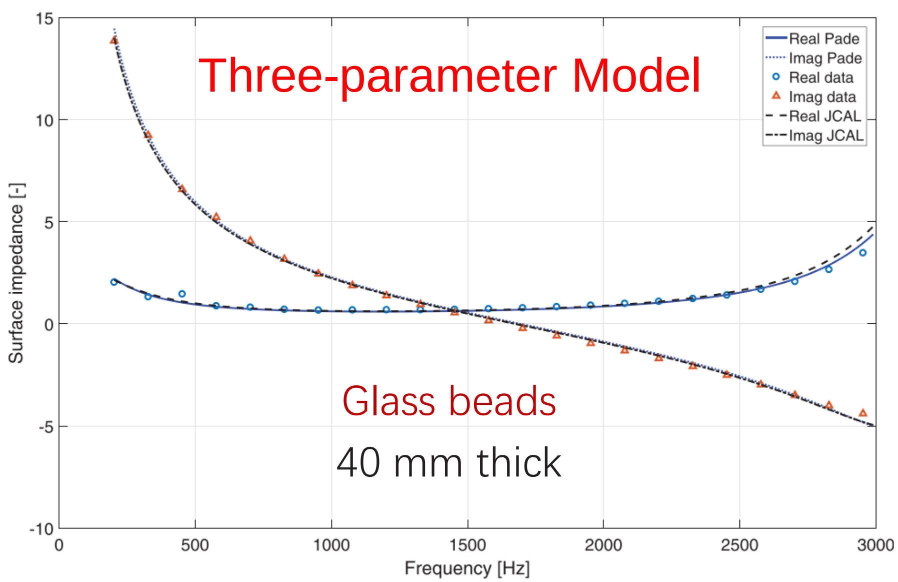

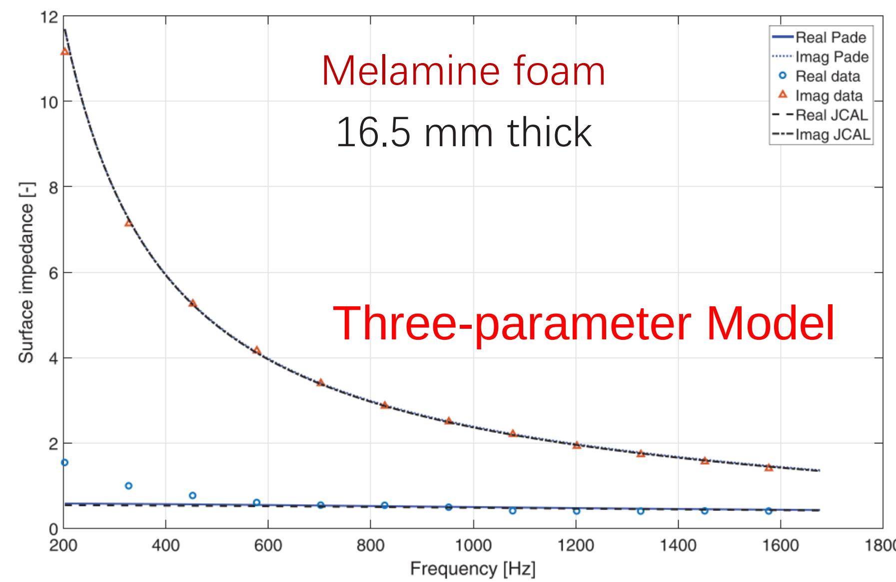

Acoustic absorption performance of CNCAs

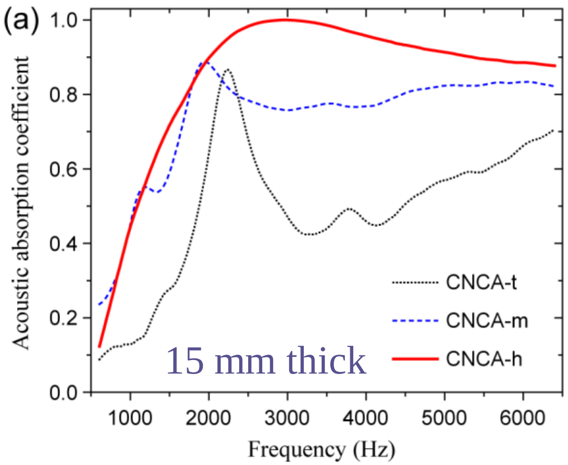

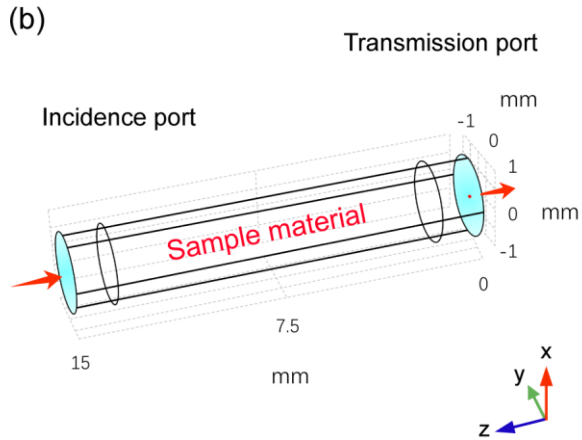

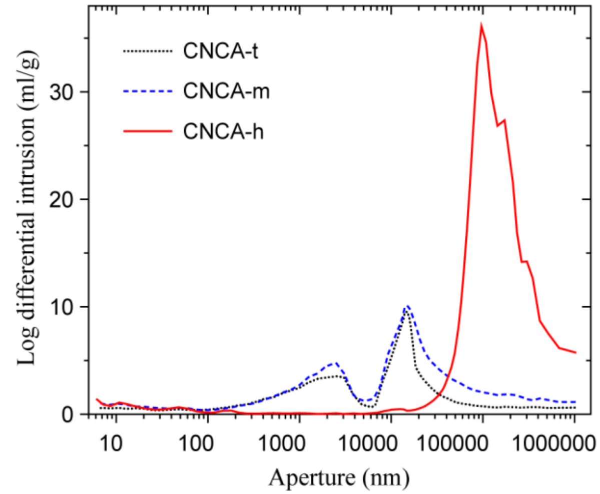

Fig. 11. (a) Normal acoustic absorption coefficient of CNCAs. (b) Schematic of the designed porous media model to predict the acoustic absorption behavior.

Pore size distribution

Table. 4. Characteristics of the porous structure of CNCAs

	CNCA-t	CNCA-m	CNCA-h
Average aperture (um)	0.19	0.19	0.45
Most probable aperture (um)	14.91	14.90	96.19
Permeability (Darcy)	0.32	19.54	50.03
Porosity (%)	94.29	95.07	97.62
Density (g/cm^3)	0.087	0.075	0.036

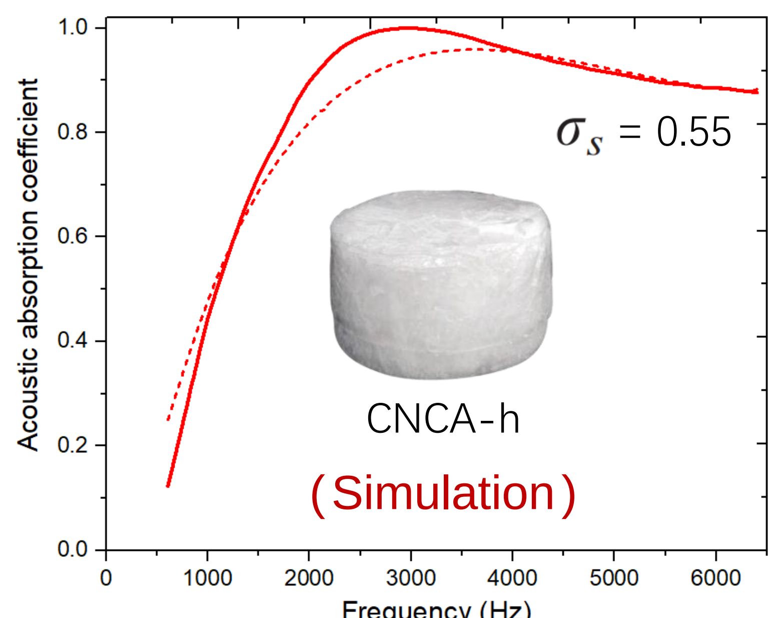

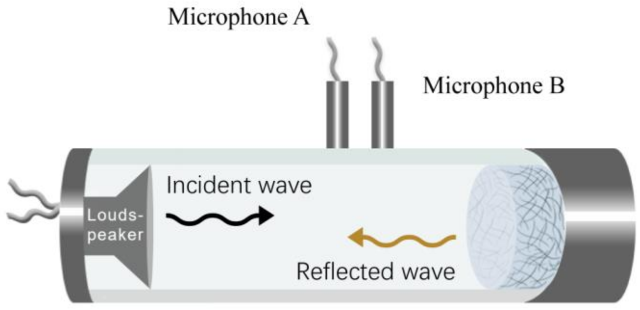

‘Impedance tube method’

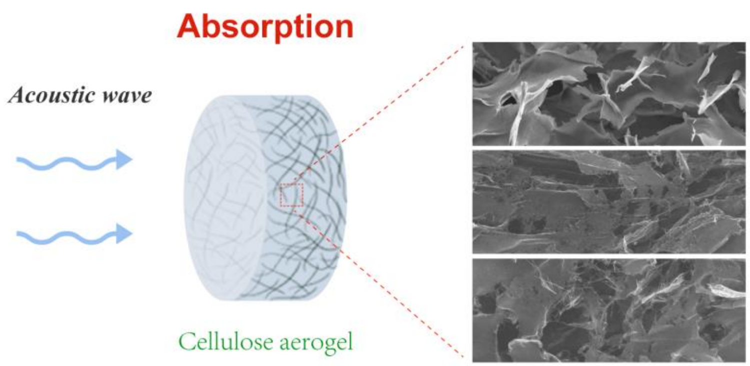

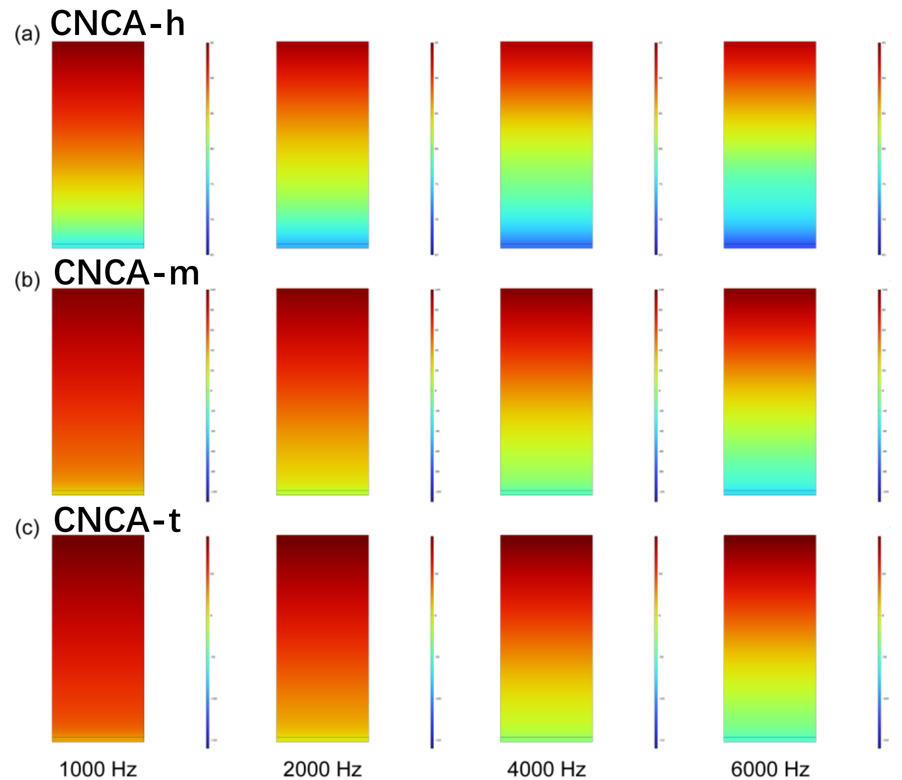

Sound pressure level [dB]

Table. 5. Acoustic absorption performance of CNCAs

	Average absorption coefficient A_{ave}	Maximum absorption coefficient A_{max}	Bandwidth **BW** (Hz)
CNCA-t	0.49	0.87	225
CNCA-m	0.74	0.89	2514
CNCA-h	**0.85**	**0.99**	**4673**

Multi-functionality of CNCAs

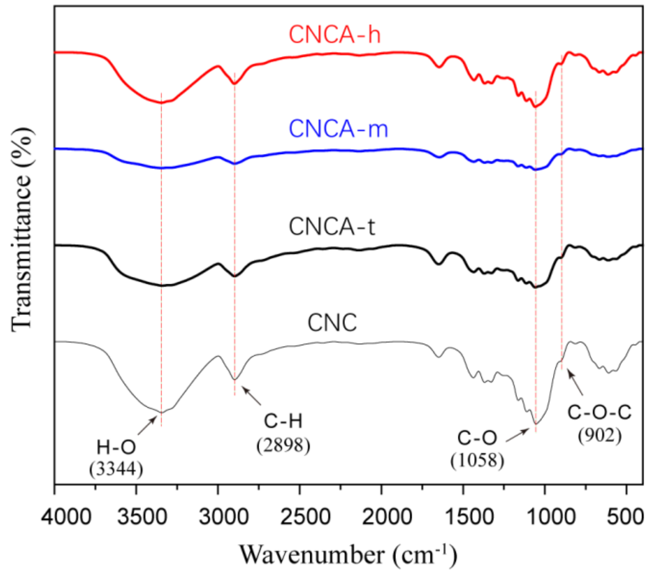

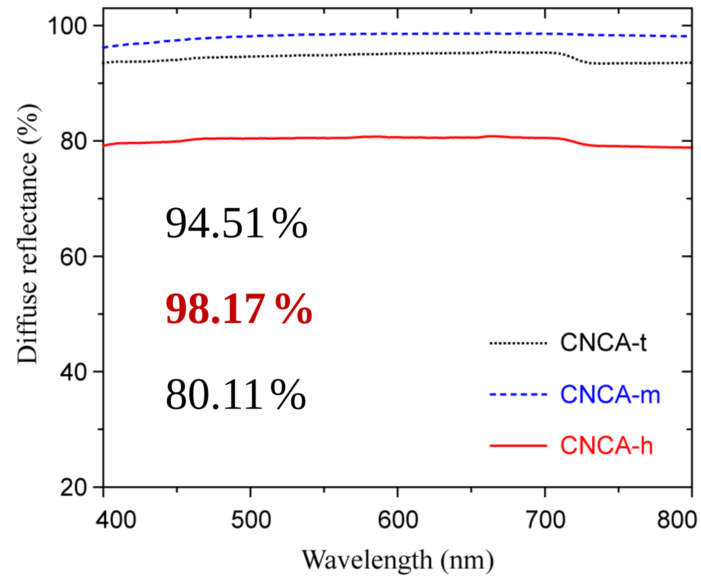

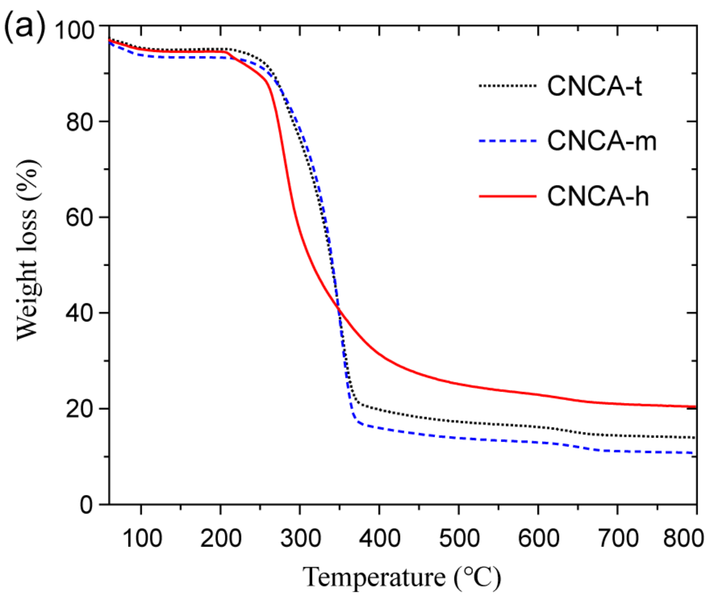

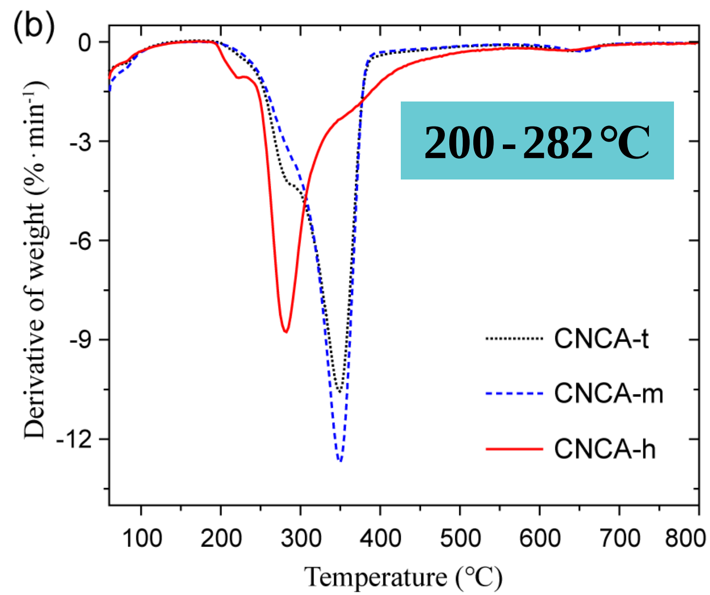

4. Summary and Outlook

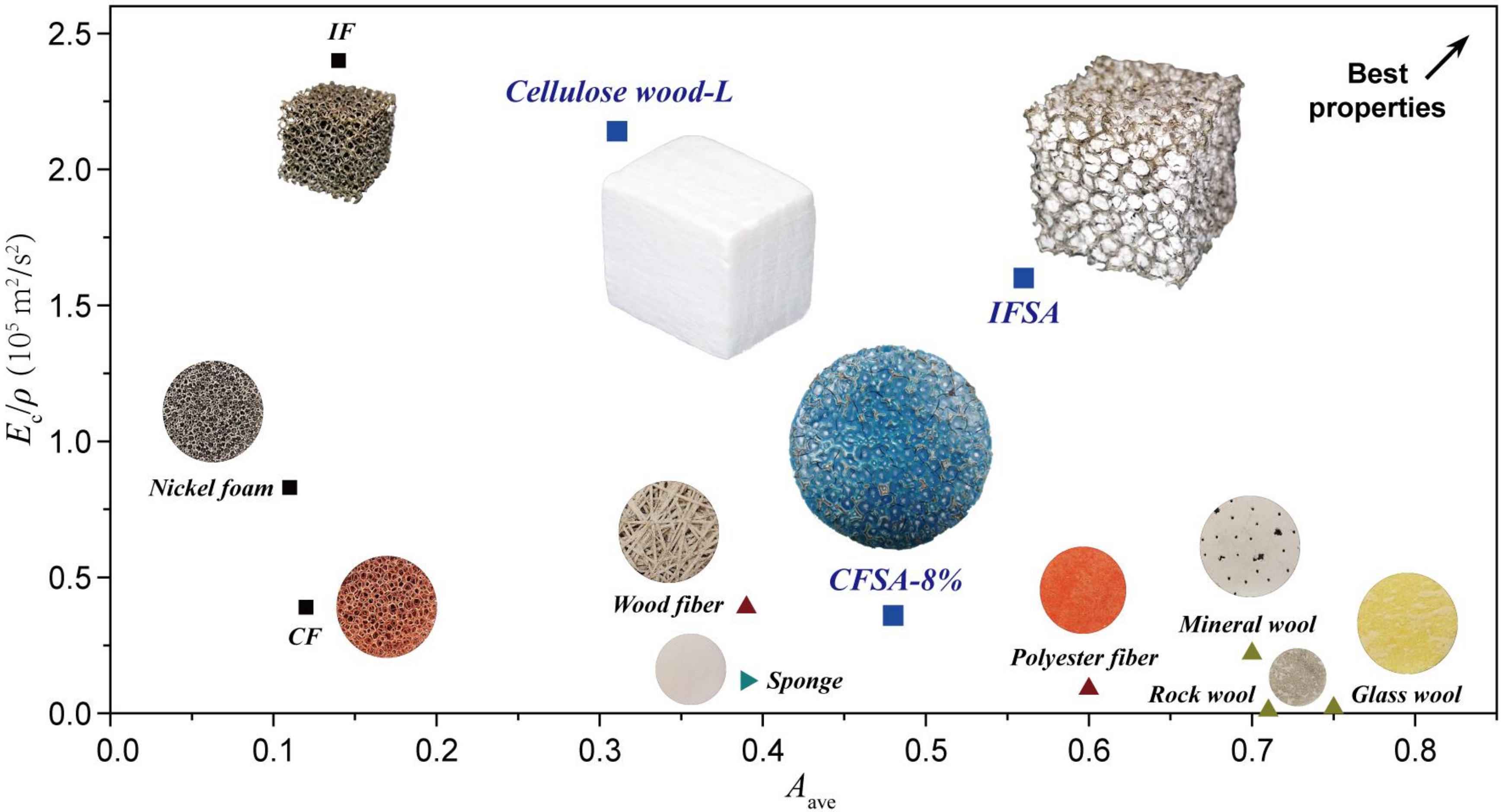

Acoustics ⟷ **Mechanics**

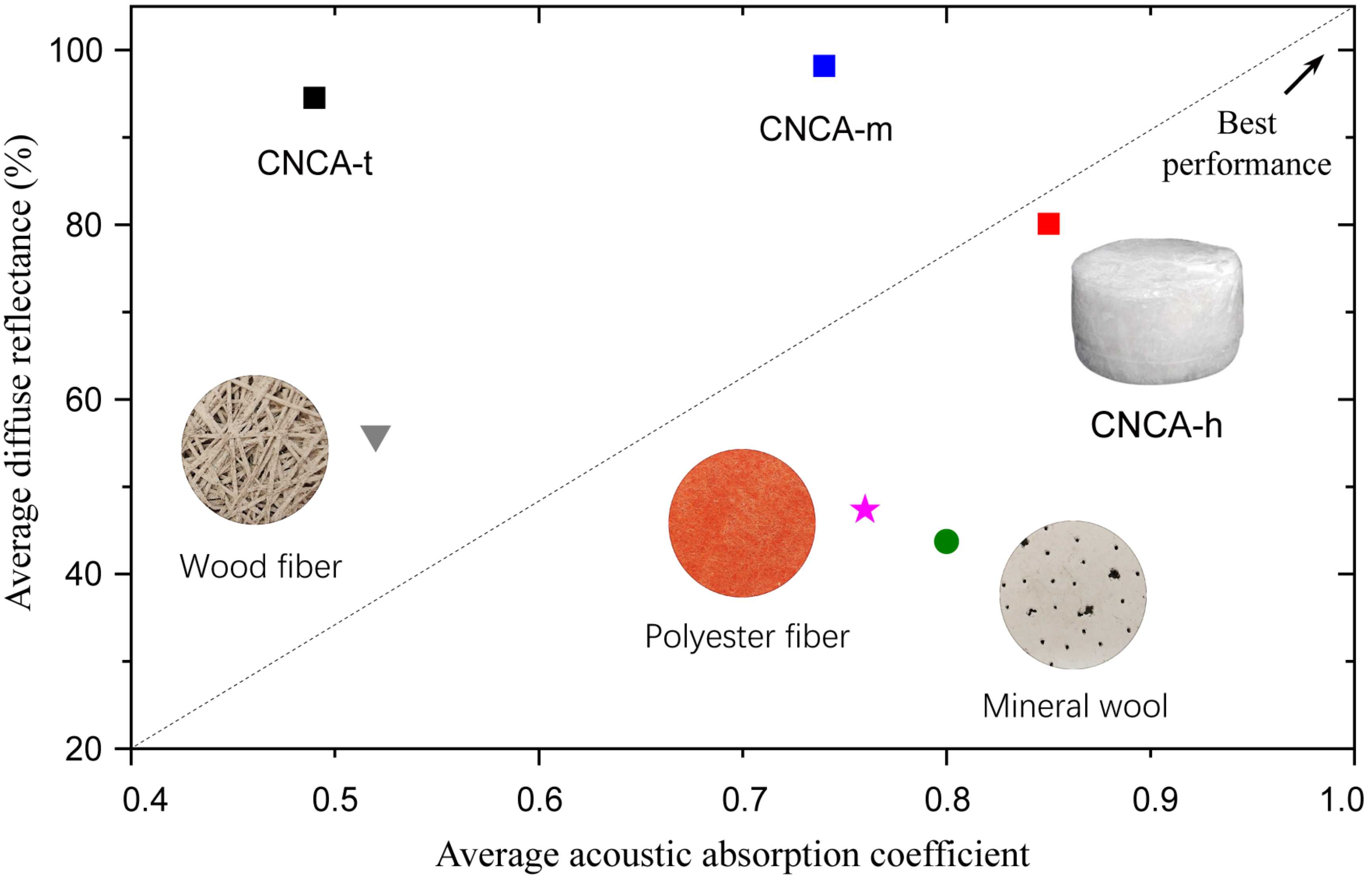

Acoustics ⟷ Optics

Metal Foam/Aerogel Composites

Novel Lightweight & Multifunctional Structural Material

High Efficiency for Noise Reduction
Energy Saving & Emission Reduction


Aeronautics & Astronautics

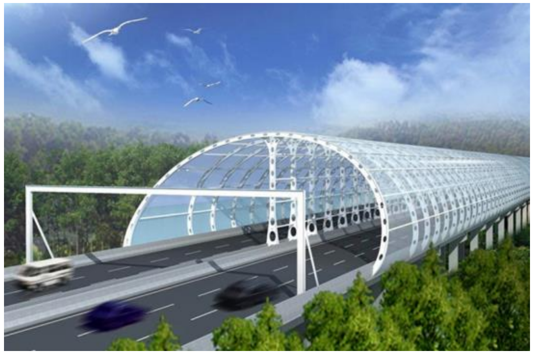
Rail Transit


Constructions

Biobased Aerogels

Novel Multifunctional Indoor Material

Quiet	Brightness
Health	Comfort

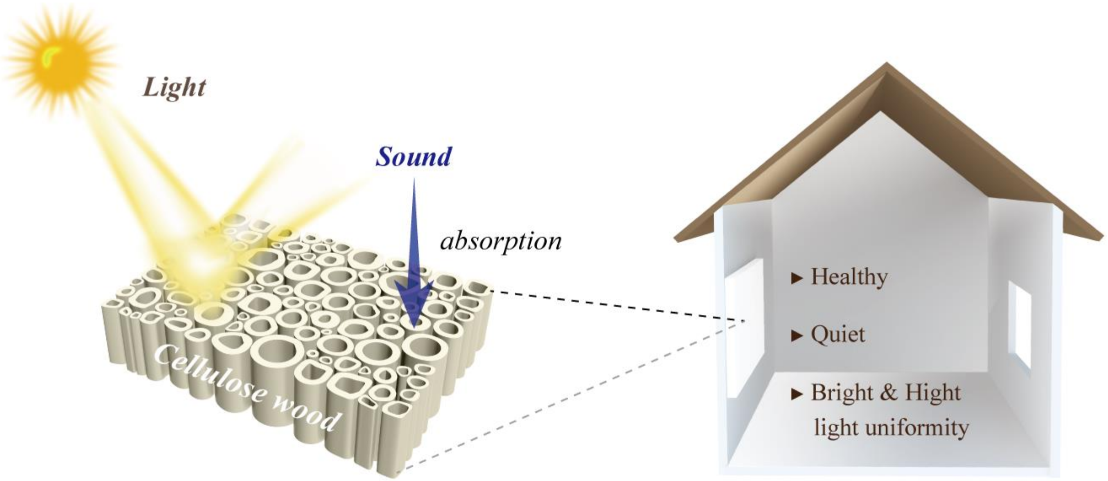

Publications Related to This Report

► Ju-Qi Ruan, Kai-Yue Xie, Zhaoxi Li, Xiaoqing Zuo, Wei Guo, Qing-Yuan Chen, Houyin Li, Chunlong Fei, and Ming-Hui Lu, Multifunctional ultralight nanocellulose aerogels as excellent broadband acoustic absorption materials. *Journal of Materials Science* **58**: 971-982 (2023) (**Editor's Pick**)

► Ju-Qi Ruan, Zhaoxi Li, Kai-Yue Xie, Wei Guo, Chunlong Fei, Ming-Hui Lu, and Hai Yang, Multifunctional cellulose wood with effective acoustic absorption. *AIP Advances* **12**: 055102 (2022)

► Ju-Qi Ruan, Shahrzad Ghaffari Mosanenzadeh, Xin Li, Si-Yuan Yu, Chu Ma, Xin Lin, Shan-Tao Zhang, Ming-Hui Lu, Nicholas X. Fang, and Yan-Feng Chen. Bimodal hybrid lightweight sound-absorbing material with high stiffness. *Applied Physics Express* **12**: 035002 (2019) (**Editor's Pick**)

► Ju-Qi Ruan, Hao Ge, Dafang Huang, Xin Li, Shan-Tao Zhang, and Ming-Hui Lu, Copper foam sustained silica aerogel for high-efficiency acoustic absorption. *AIP Advances* **9**: 015209 (2019)

► 卢明辉, 阮居祺, 李政, 张善涛, 陈延峰, 基于环氧树脂增强的泡沫金属/二氧化硅气凝胶复合吸声材料的制备方法. 专利号: ZL 2015 1 0810252.5 (中国发明专利)

► 崔升, 阮居祺, 沈晓冬, 一种亲水型SiO_2气凝胶的制备方法. 专利号: ZL 2013 1 0287903. 8 (中国发明专利)

Acknowledgements

Prof.
Yan-feng Chen

Prof.
Ming-Hui Lu

Prof.
Ming-Wei Zhu

Prof.
Sheng Cui

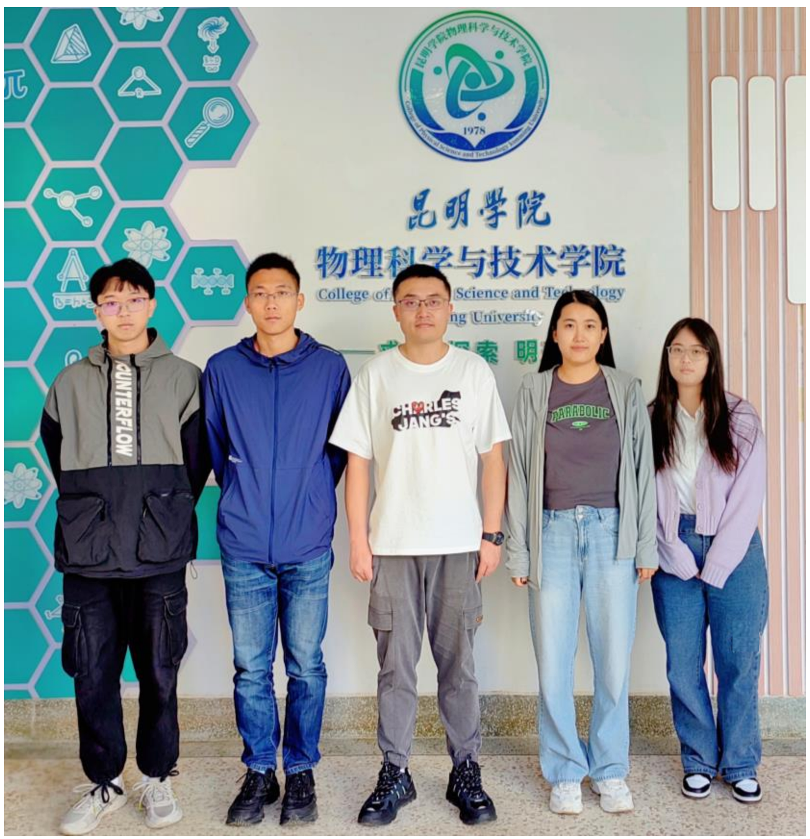

The above researches were supported by:

- ► **Yunnan Fundamental Research Projects** (Grant No. 202201AU070036, No. 202101BA070001-175)
- ► **National Natural Science Foundation of China** (Grant No. 52261009)
- ► **Science Foundation of Kunming University** (Grant No. YJL20014)
- ► **Science Foundation of the National Laboratory of Solid State Microstructures** (Grant No. M35032)

附　录

Acoustic absorption performance of CWs

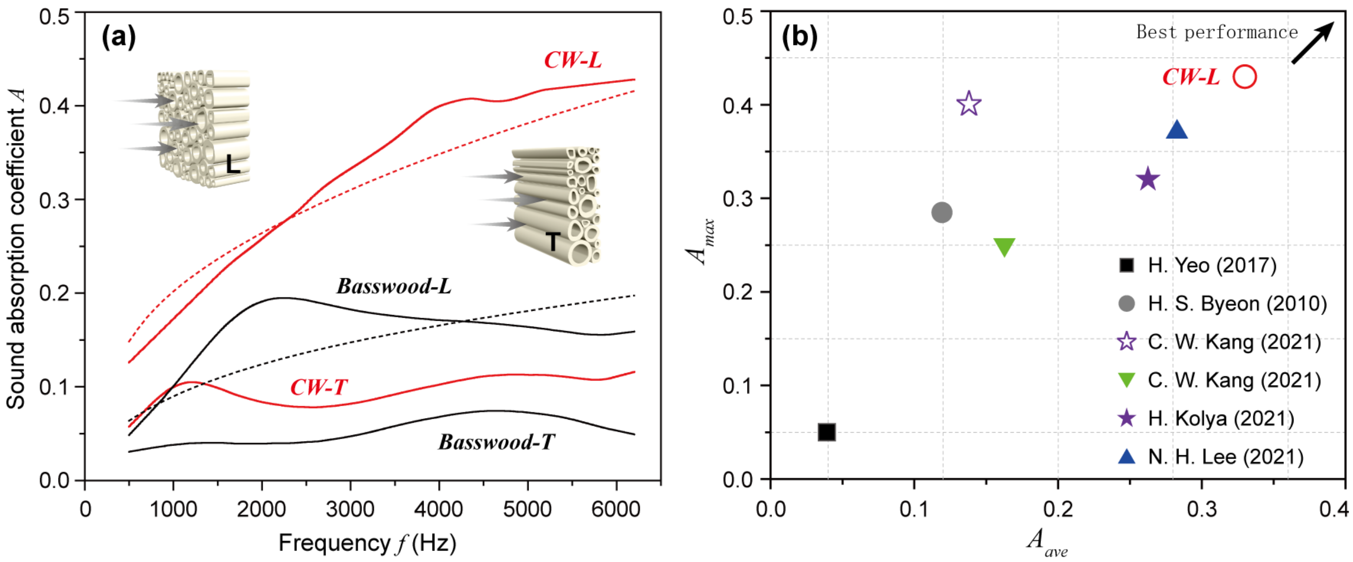

Fig. 10. (a) Normal incident sound absorption coefficient of natural basswood and CWs. (b) Comparison of the acoustic absorption performance.

ϕ	75.47%	87.07%
$\bar{S}$	0.58	1.01
σ_s	0.97	1.01

Table. 3. Air permeability and acoustic absorption performance of natural basswood and CWs

	Air permeability (Darcys)	A_{ave}	A_{max}
Basswood-T	0.34	0.05	0.07 (at 4600 Hz)
Basswood-L	5.66	0.16	0.19 (at 2280 Hz)
CW-T	0.53	0.10	0.12 (at 6180 Hz)
CW-L	33.78	0.33	0.43 (at 6120 Hz)

Cellulose wood

★ 环氧树脂掺入量对 SA 结构的影响

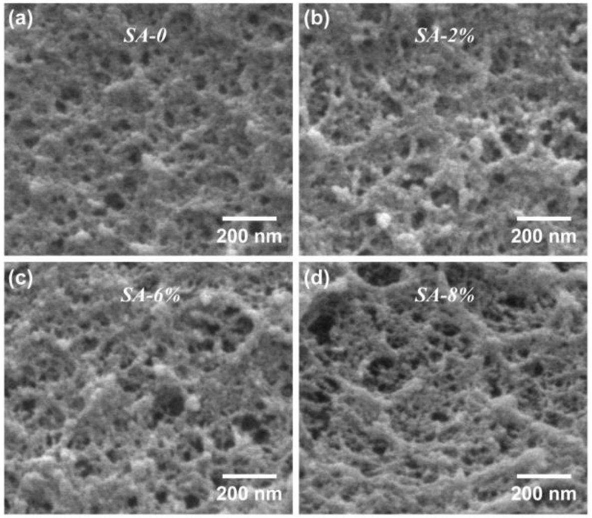

环氧树脂掺入量对 SA 微观形貌的影响

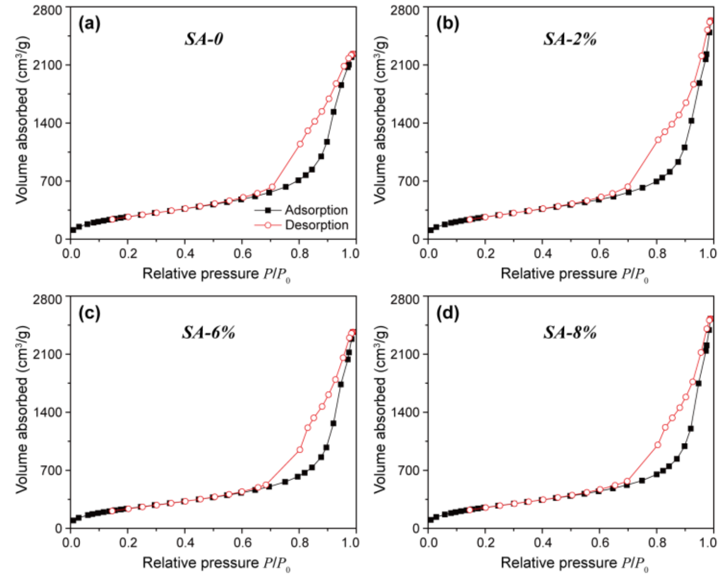

不同环氧树脂掺入量的 SA 的 N_2 吸附-脱附等温线

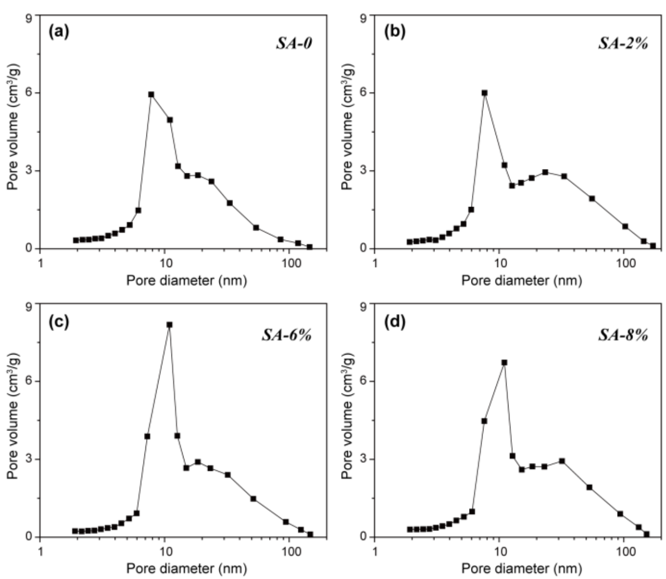

环氧树脂掺入量对 SA 孔径分布的影响

环氧树脂掺入量对 SA 孔结构参数的影响

Sample	SA-0	SA-2%	SA-6%	SA-8%
Specific surface area (m^2/g)	1033.68	1026.74	920.71	969.99
Total pore volume (cm^3/g)	3.20	3.35	3.15	3.31
Average pore size (nm)	124.00	130.69	136.86	136.56

结论：适量掺入环氧树脂不会破坏 SA 优越的孔结构。

★ 双模结构

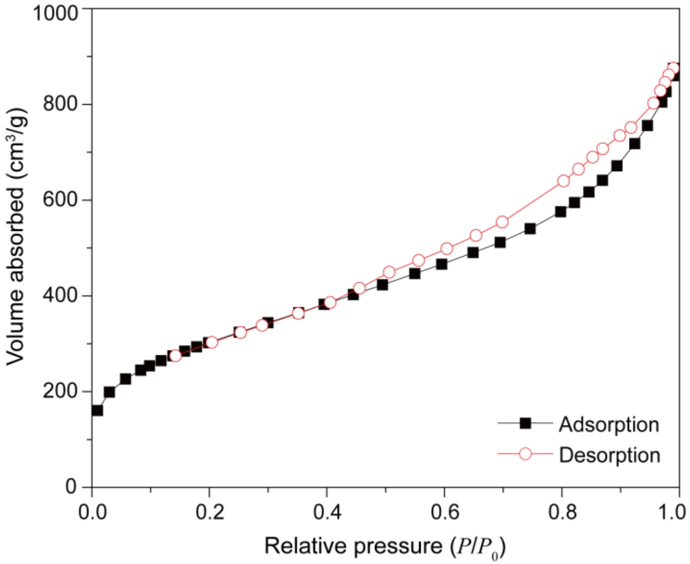

SA 的 N_2 吸附-脱附等温线

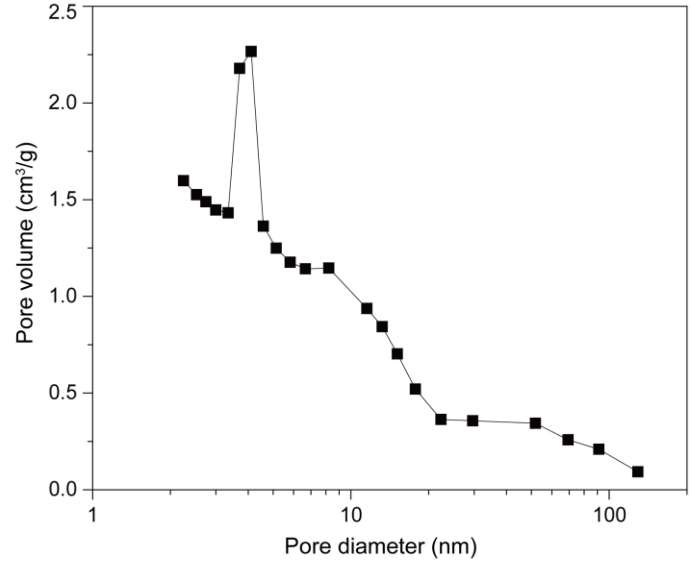

SA 的孔径分布

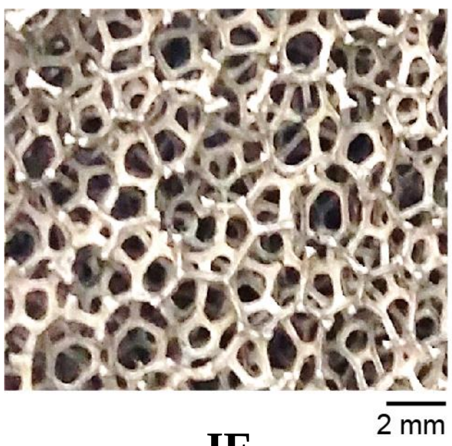

IF
初级结构

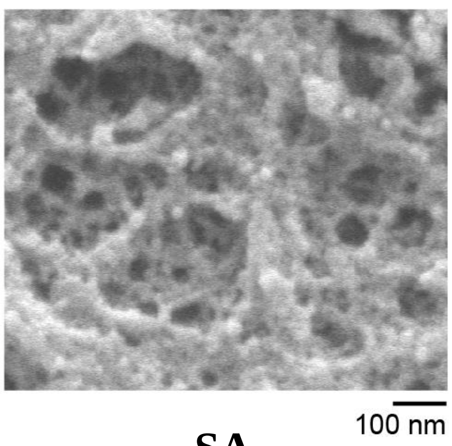

SA
二级结构

- ► Specific surface area 1106.44 m^2/g
- ► Total pore volume 1.24 cm^3/g
- ► Average pore size 4.5 nm

结论：经冷冻干燥制备的 SA 呈现出优越的孔结构。

★ 纤维素木头的结构

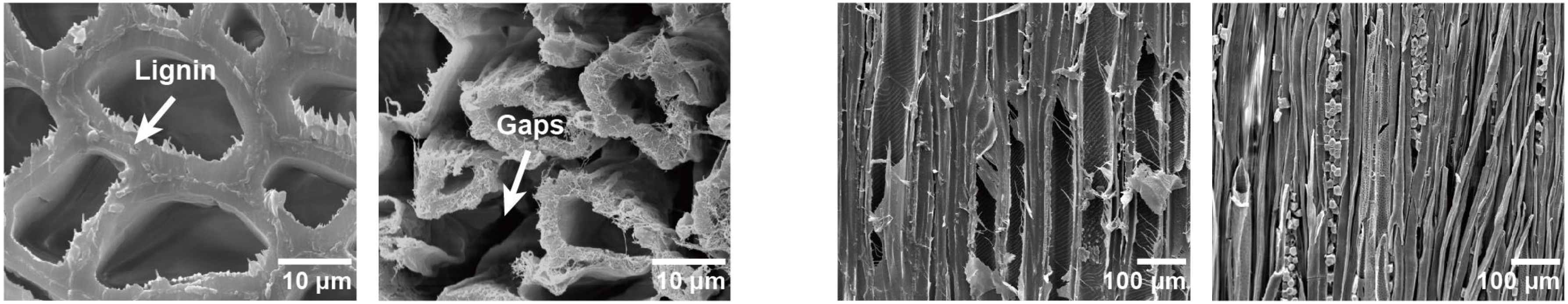

Natural basswood-L **Cellulose wood-L** **Natural basswood-T** **Cellulose wood-T**

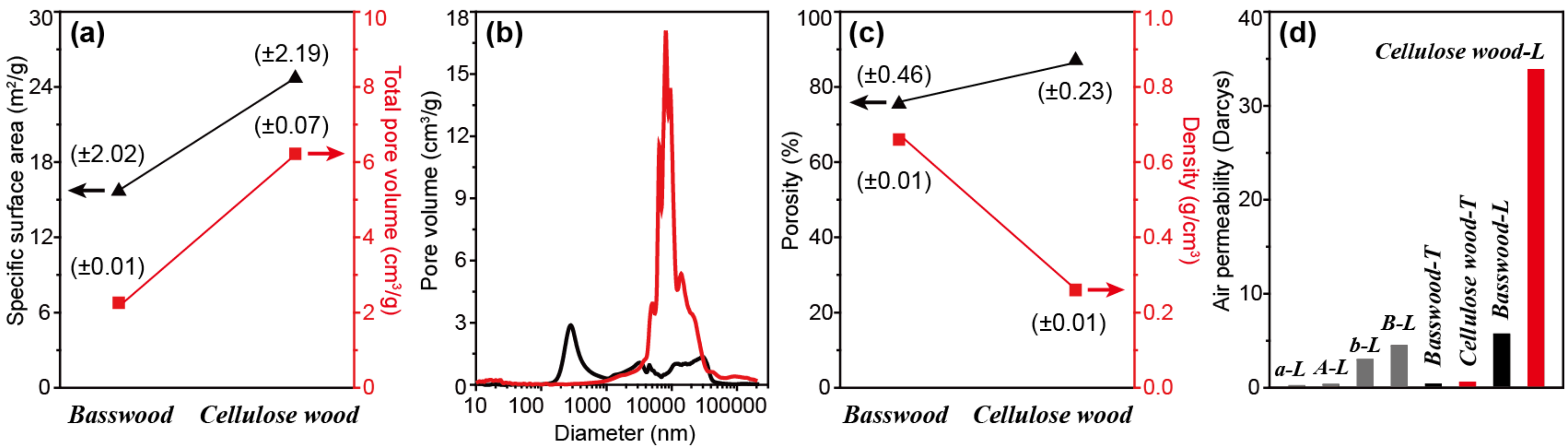

天然椴木与纤维素木头结构通透性对比。其中 “a-L” 为日本落叶松，“ A-L” 为去除木质素后的日本落叶松 [1]；“ b-L” 为北美鹅掌楸，“ B-L” 为经汽爆处理后的北美鹅掌楸 [2]。

去除木质素 —提高→ **结构通透性**

[1] C. W. Kang, et al., *J. Fac. Agr. Kyushu Univ.* 53, 479-483 (2008).
[2] C. W. Kang, et al., *J. Fac. Agr. Kyushu Univ. 55*, 327-332 (2010).

★ 纤维素木头的准静态压缩性能

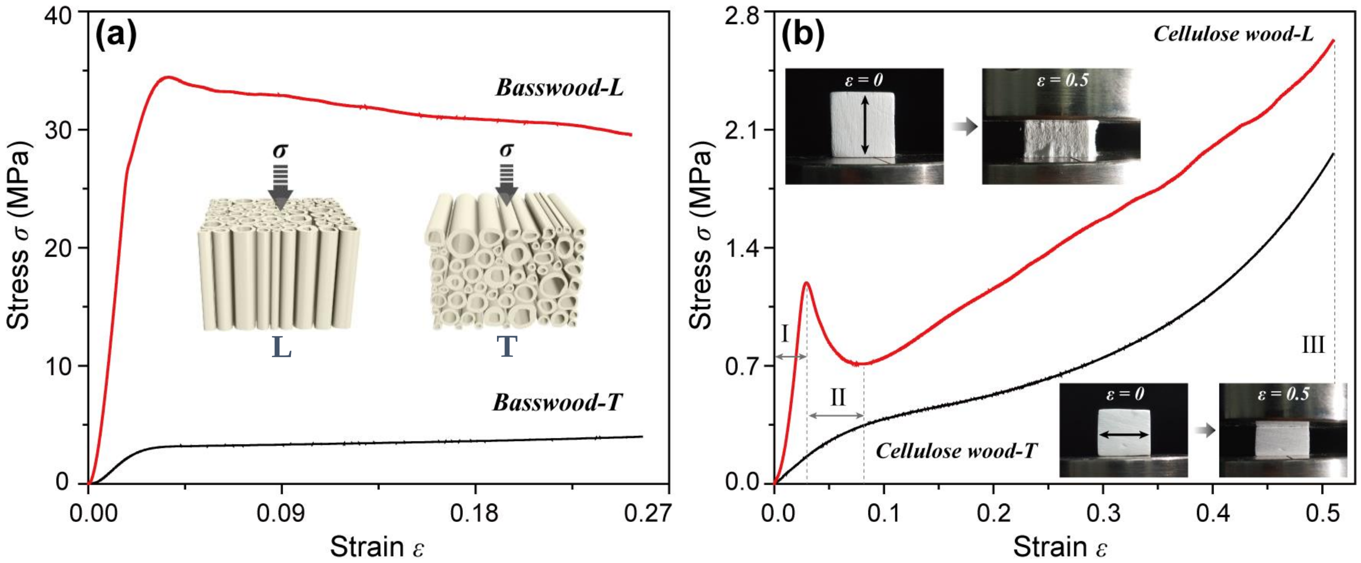

天然椴木和纤维素木头的轴向准静态压缩应力-应变曲线

I 线弹性阶段
($\varepsilon < 0.03$)

II 塑性形变阶段
($0.03 < \varepsilon < 0.08$)

III 致密化阶段
($\varepsilon > 0.08$)

天然椴木和纤维素木头的抗压性能参数

Sample	Young's modulus E_c (MPa)	Compression strength σ_c (MPa)	Specific modulus E_c / ρ (10^5 m^2/s^2)
Basswood-T	146.1	3.2	2.21
Cellulose wood-T	5.34	0.53	0.21
Basswood-L	1679.53	34.44	25.45
Cellulose wood-L	55.55	1.19	2.14

结论： 纤维素木头一定程度上保留了天然椴木优越的抗压性能，具备较高的杨氏模量、抗压强度和比模量。

★ 纤维素木头的漫反射特性

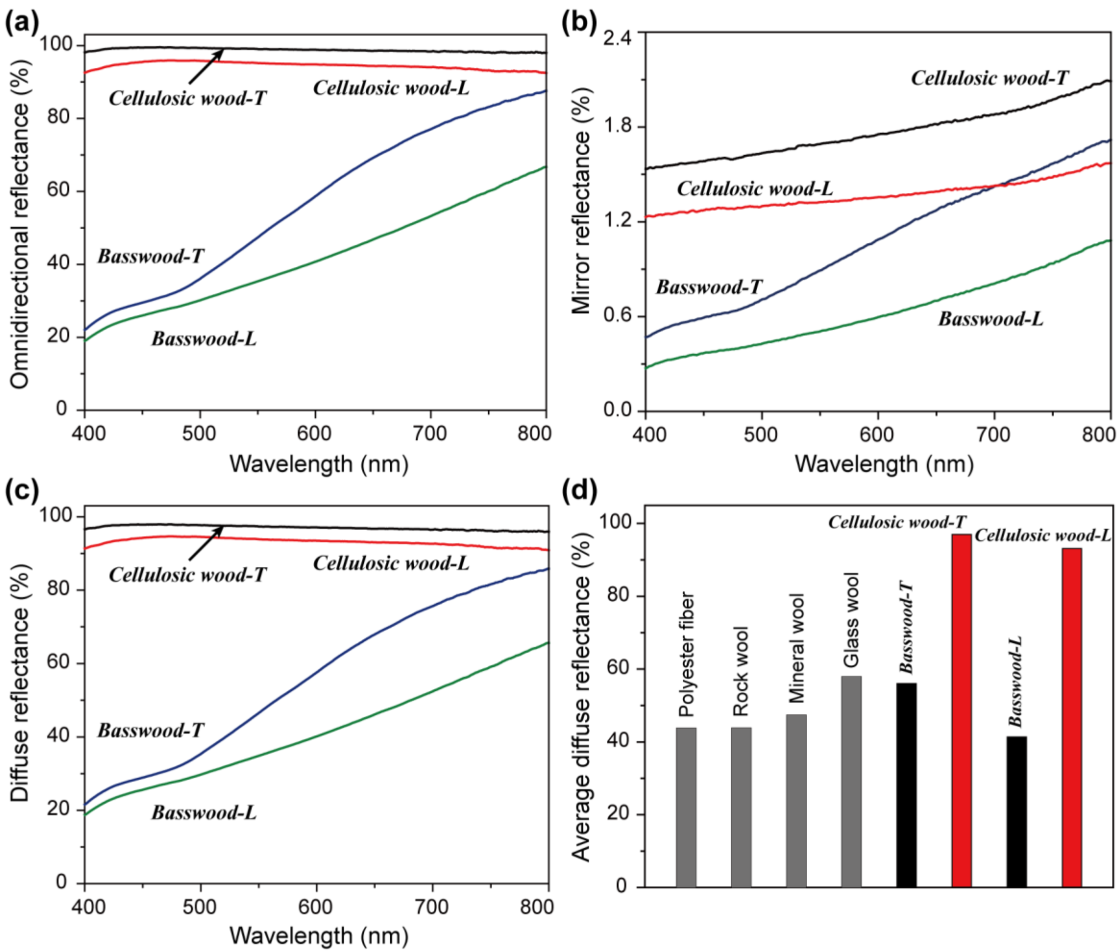

天然椴木和纤维素木头的 (a) 全反射、(b) 镜面反射和 (c) 漫反射性能；(d) 纤维素木头与天然椴木，以及一些常见吸声材料平均漫反射系数的对比。

去除木质素

纳米散射中心 [1,2]

[1] L. Hu, et al., *Energy Environ. Sci.* 6, 513-518 (2013).
[2] Z. Wu, et al., *Angew. Chem.* 125, 2997-3001 (2013).

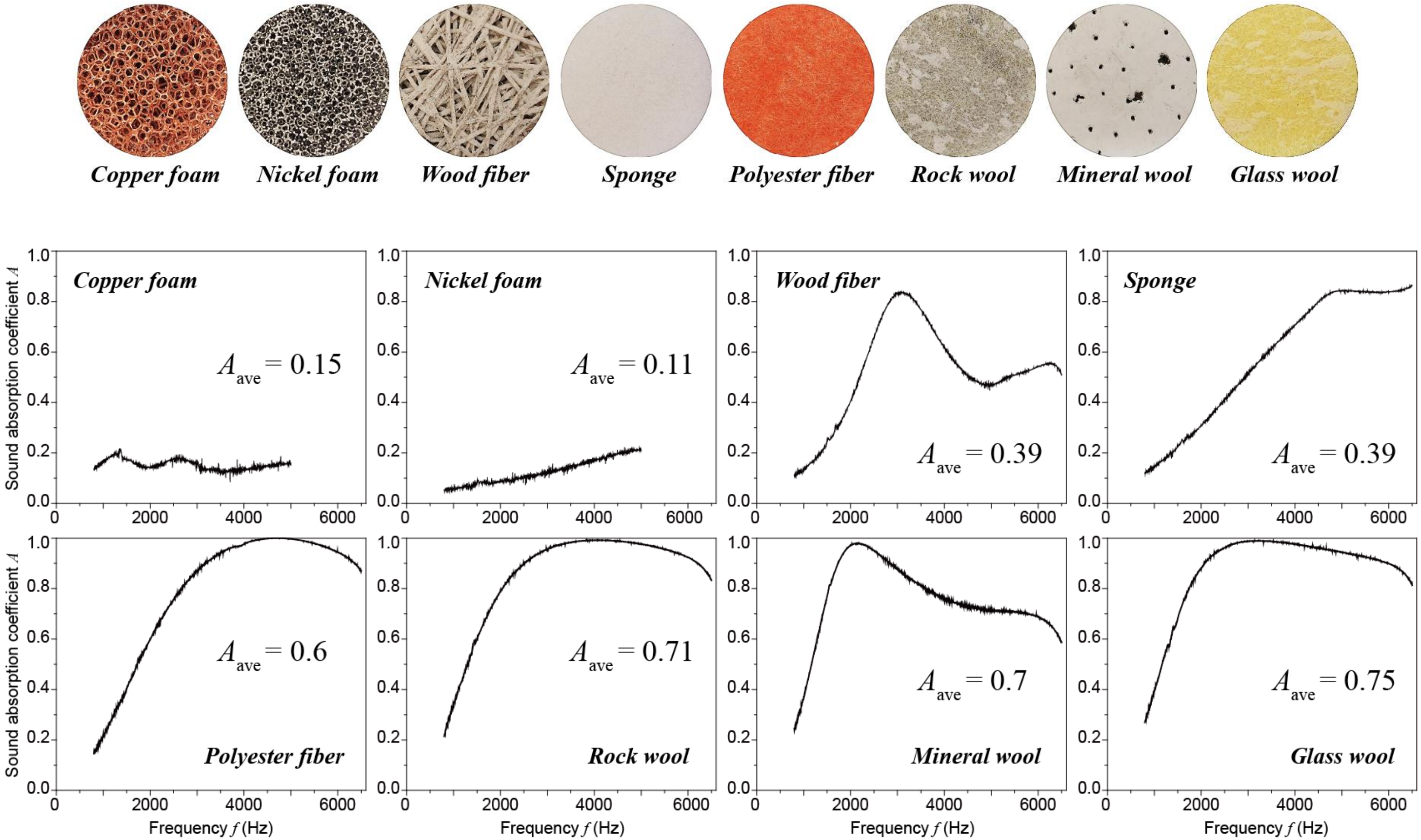

几种常见吸声材料的吸声性能（样品厚度为15 mm）

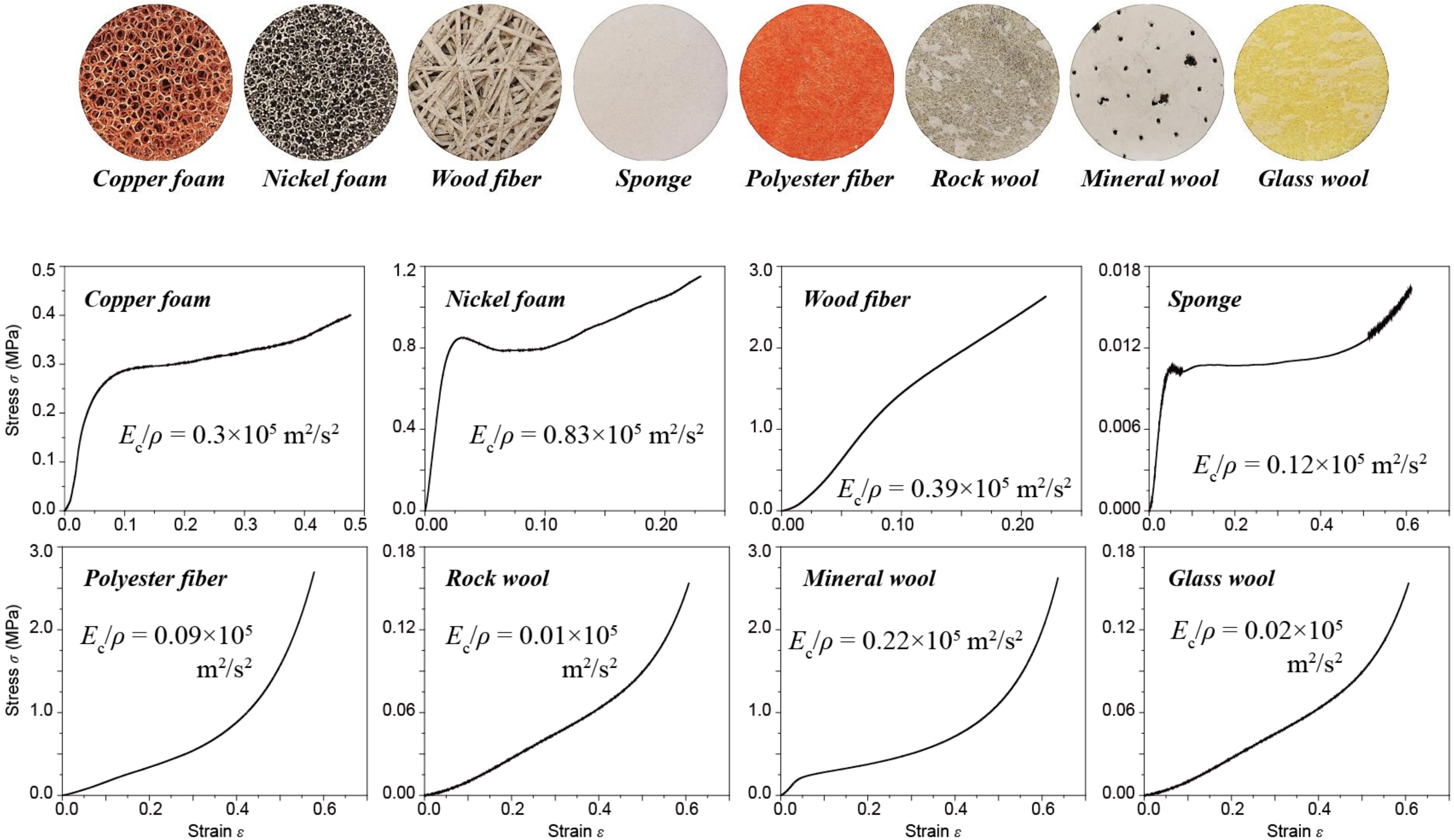

几种常见吸声材料的抗压性能（压缩速率为 0.5 mm/min）

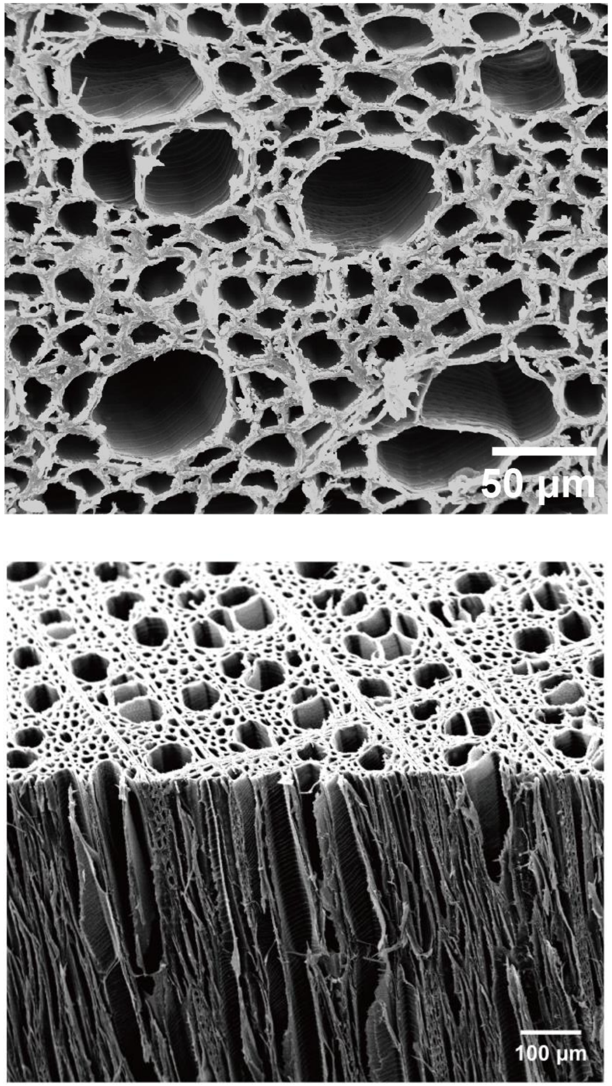

天然椴木

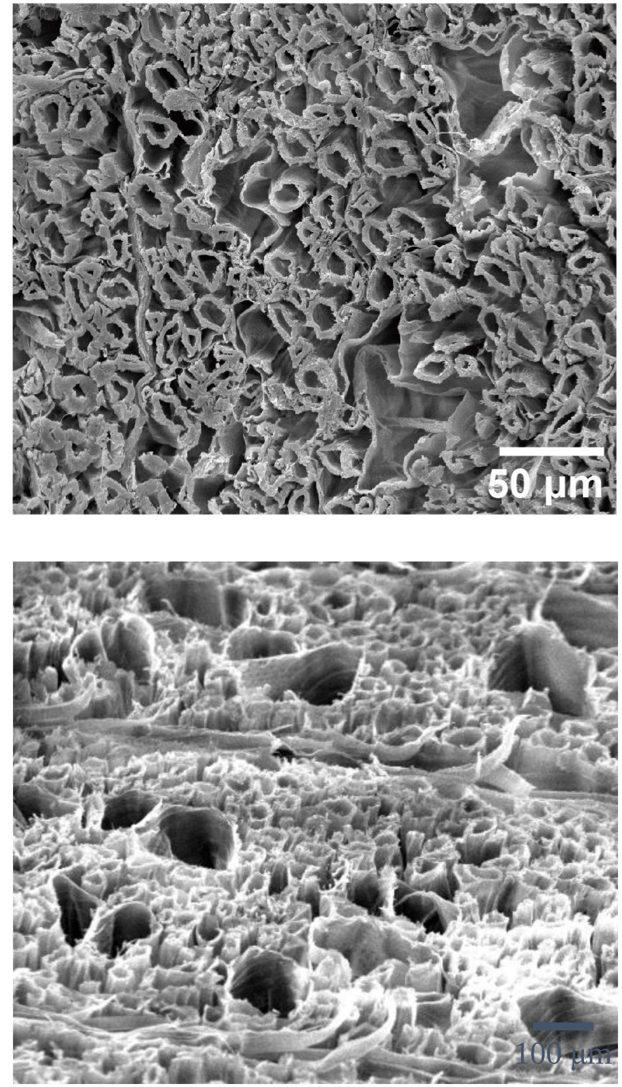

纤维素木头

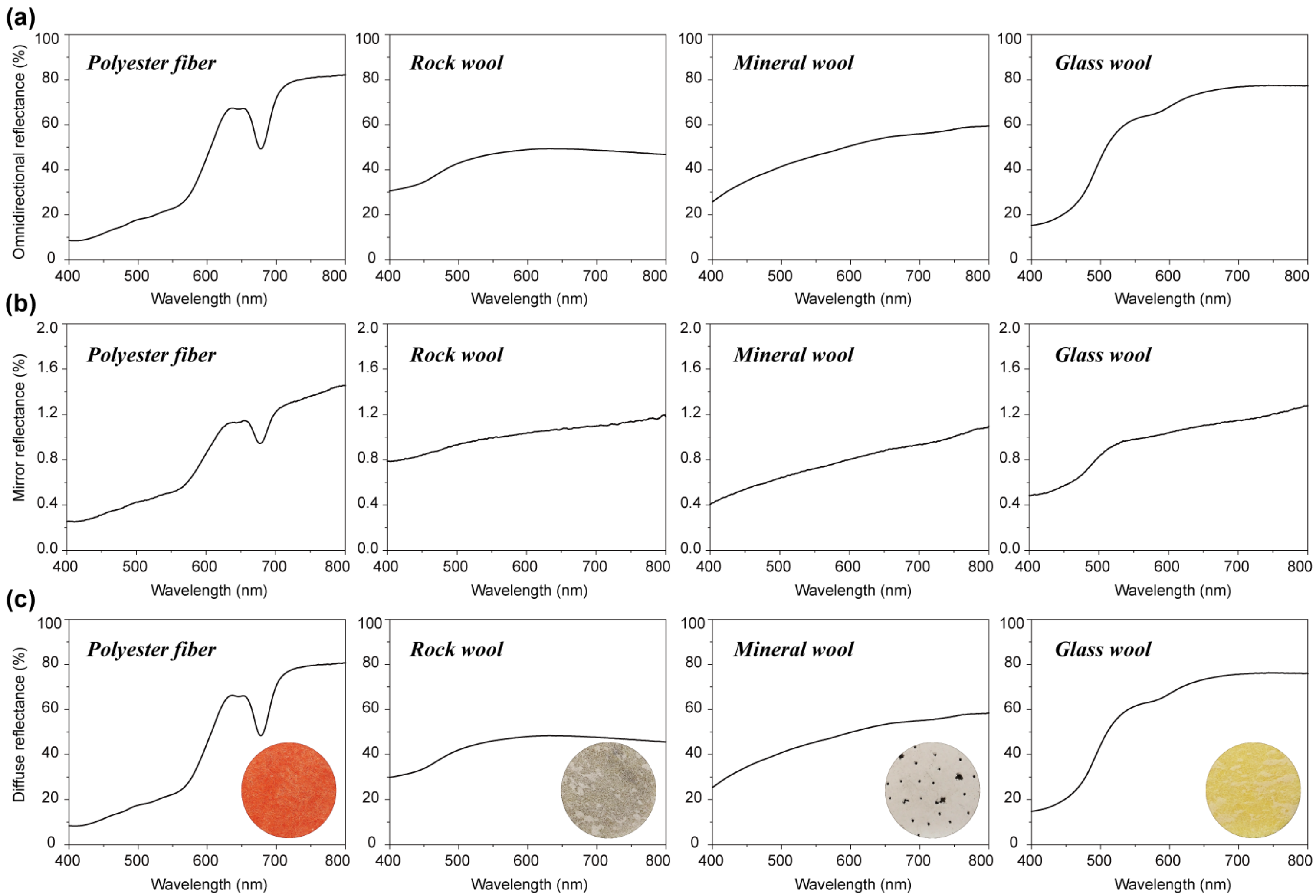

一些常见吸声材料的 (a) 全反射性能；(b) 镜面反射性能和 (c) 漫反射性能